FURTHER CHARACTERIZATION OF METACASPASE EXPRESSION AND ACTIVITY IN MARINE PHYTOPLANKTON

by

WANJING LIAO

A thesis submitted to the

Graduate School-New Brunswick

Rutgers, The State University of New Jersey

in partial fulfillment of the requirements

for the degree of

Master of Science

Graduate Program in Oceanography

written under the direction of

Kay D. Bidle

and approved by

_____

_____

_____

New Brunswick, New Jersey

[January, 2010]

ABSTRACT OF THE THESIS

FURTHER CHARACTERIZATION OF METACASPASE EXPRESSION AND ACTIVITY IN MARINE PHYTOPLANKTON

By WANJING LIAO

Thesis Director:

Kay D. Bidle

Metacaspases are considered to be ancestral cysteinyl aspartate specific proteases involved in the initiation and execution of apoptotic programmed cell death (PCD). The widespread presence of metacaspases genes among a variety of phytoplankton, suggests that they play a fundamental role in cell turnover, aquatic food webs, and biogeochemical cycles. Yet, there are still fundamental questions that exist about these enzymes: How does metacaspase diversity relate to different evolutionary plastid lineages? What is their relationship to cell physiology? Are metacaspases associated with caspase activity?

Using hydrolysis of a fluorogenic canonical tetrapeptide substrate and western blot analysis, we report on the induction of caspase-like activity and metacaspases-like

protein expression from four ecologically and evolutionarily diverse phytoplankton species, including a chlorophyte (*Dunaliella tertiolecta*), a haptophyte (*Isochrysis galbana),* a diatom (*Thalassiosira weissflogii*), and a dinoflagellate (*Amphidinium carterae*). These derived eukaryotic lineages represented phytoplankton from primary (*D. tertiolecta*), secondary (*I. galbana* and *T. weissflogii*), and tertiary endosymbiotic (*A. carterae*) events. Immunohybridization to polyclonal antisera raised against a coccolithophore metacaspase indicated high conservation of caspase-like proteins and an accumulation of metacaspase complexity with evolutionary complexity.

An *E. huxleyi CCMP1516* (*Ehux1516*) and EhV86 host-virus model system was used to link dramatic increases in caspase specific activity with protein signatures via a genome-enabled, proteomic approach. Both the host and virus have sequenced genomes and EhV86 strongly triggered caspase activity. Caspase activation was measured through *in vitro* cleavage of fluorogenic peptide substrates with up to ~170-fold increase during infection. Subsets of partially purified proteins were associated with enhanced caspase specific activity and displayed hybridization to metacaspase antibodies. Pooled subsets of caspase active fractions from size exclusion chromatography were subjected to both 1D SDS-PAGE and 2D gel electrophoresis (GE) followed by mass spectrometry analysis. SYPRO-Ruby staining of 2D gels yielded approximately 10-17 clearly definable protein spots for caspase active fractions. Seventeen proteins hits, including four from the EhV86 proteome, were homologues to proteases or death related proteins, suggesting these proteins may be responsible for

observed caspase activities and some may be virally derived. Further work should focus on validating the activity and function of these gene products.

ACKNOWLEDGEMENTS

First and foremost I want to express my deepest gratitude to my advisor Prof. Kay Bidle, for the source of knowledge, mentoring, and support that he has been to me through my graduate career. I appreciate all that I have learned from him in the lab and in the classroom. He is the most wonderful professor, down to Earth, who wants you to succeed.

I owe many thanks to my committee for helping shape this thesis: Prof. Paul Falkowski and Prof. Oscar Schofield. Thanks for taking the time to serve on my thesis committee and their advice throughout the writing process.

My research could not have been completed without the help of the entire Bidle Lab and Environmental Biophysics and Molecular Ecology (EBME) group, including Assaf Vardi, Chris Brown, Kim Thamatrakoln, Liti Haramaty, Frank Natale, Matthew Johnson, Miguel Frada, Kevin Wyman, Yael Helman, Adam Kustka, Marta Sebastian, Chengyi Yan, Yi Xu, Hui Liu, Xiaona Li, Olga Korenovska, and Clifford Kwityn. It has been a pleasure to work with such brilliant people, and I am honored to have called them colleagues.

I would also like to acknowledge all the IMCS faculty, researchers, graduate students who taught me classes, answered my questions. From these people here, I really learned a lot about what I do for a living. It’s really being an education.

Special thanks also go to the entire IMCS staff, especially Beatrice Birrer, Yana Zeltser, Lynn Demenchuk, Sarah Kasule, and Lillian Lee.

I thank the Chinese friends in Cook College, for making the days in Starkey Apt and Cook College enjoyable.

Finally, I would like to thank my parents for their love and unconditional support.

Table of Contents

LIST OF TABLES

LIST OF FIGURES

1.0 Introduction

Phytoplankton account for less than 1% of the Earth's photosynthetic biomass. However, they account for almost half of the global primary production, with net marine primary production being estimated at 48 Pg C per year (Field 1998). The high production/biomass ratio of phytoplankton in aquatic ecosystems indicates extremely high turnover rates, which means, on average, these organisms grow, die and are replaced once a week. This has important implications for the coupling of phytoplankton biomass to marine foodwebs (Bidle and Falkowski 2004). Three major ecosystem pathways "process" phytoplankton organic matter in the ocean: vertical sinking flux, grazing food chain, and the microbial loop (Fig 1.1; Bidle and Falkowski 2004). Vertical sinking flux, which is facilitated by aggregated phytoplankton cells, zooplankton faecal pellets and polymeric matter (eg. marine snow), sink irreversibly and remove the organic matter from the upper ocean into the deep ocean. The classic grazing food chain, involves phytoplankton being eaten by heterotrophic zooplankton and those zooplankton in turn are eaten by larger zooplankton and fish, with organic matter being transferred up to higher trophic levels. Lastly, the "microbial loop" is a pathway whereby dissolved organic matter (DOM) and particulate organic matter (POM) derived from photosynthesis is utilized by marine bacteria, leading to the regeneration of nutrients and biogeochemical cycling (Azam 1983).

Up until the mid-1970's, the study of biogeochemical cycles in aquatic ecosystems was based on the misconception that phytoplankton were immortal without

grazing and vertical sinking balancing phytoplankton growth. However, nearly 50% of global primary productivity flows through the microbial loop, which requires extensive death and turnover independent of sinking and grazing (Cole 1988). Extensive cell death by lysis has been documented in the decline of the *Phaeocystis* spring bloom in the Marsdiep area of the north sea of Netherlands (van Boekel 1992, Brussaard 1995), and summer phytoplankton lysis in the northwestern Mediterranean Sea (Agusti 1998). Hence, phytoplankton cell lysis appears to be the major loss factor determining algal bloom dynamics and this puts significance on the cellular mechanisms responsible. The two mechanisms implicated for grazer-independent removal processes are viral lysis and autocatalytic, programmed cell death (PCD) (Fig 1.1; Bidle and Falkowski 2004).

Viruses are the most common biological agents in the sea, numbering at 10^7 to 10^8 viruses per milliliter of surface seawater and exceeding bacterial and phytoplankton abundances by at least an order of magnitude. High production rates of viruses result in significant lysis of host cells. Through rapid decay and replenishment, they influence biogeochemical cycles and ecological processes in the upper ocean (Fuhrman 1999). Based on evidence of infected cells (via electron microscopic analyses) and viral decay rates, viruses are rapidly produced and destroy an average of 10-20% of the heterotrophic bacteria in marine surface waters and 5- 10% of the cyanobacteria daily (Wilhelm and Suttle 1999). Viruses or virus–like particles have also been reported since the 1970's to infect eukaryotic algae phytoplankton, including *Micromonas pusilla* (Mayer and Taylor 1979, Cottrell and Suttle 1991), *Aureococcus anophagefferens* (Milligan and Cosper 1994), *Chrysochromulina spp.* (Suttle and Chan

1995), *Phaeocystis pouchetii* (Jocobsen et al. 1996), and *Heterosigma akashiwo* (Nagasaki and Yamaguchi 1997). The first isolation of an *Emiliania. huxleyi*-specific virus by plaque assay was reported in 1996. Since then, numerous viruses specific to *E. huxleyi* have been isolated (Schroeder 2002, Bratbak 1993, Bratbak 1996, Wilson 2002 and Castberg 2001), and this new virus genus *Coccolithovirus*, from the family *Phycodnaviridae*, has become the most studied phytoplankton-virus system to date. Numerous sensitive strains and both sensitive and resistant hosts strain were studied in the field and laboratory (Table 1.1, Schroeder 2002).

1.1 Programmed cell death in unicellular phytoplankton

PCD is an irreversible, genetically controlled form of cell suicide that is essential for the proper development, function and ultimate survival of metazoan organisms (Leist 1997). In contrast, the term “necrosis” is known as a passive, indiscriminant, degenerative process that often follows irreversible injury, is not characterized by *de novo* protein synthesis and ends in immediate rupture and lysis of the cells (Kerr et al. 1972, Walker et al.1988). PCD is an organized sequence of events used to dispose of unwanted or injured cells for proper development, tissue turnover, function and survival. It has long been regarded as a proprietary characteristic of metazoans (Leist 1997). However, recent laboratory studies indicate autocatalytic cell death has been identified in both prokaryotic and eukaryotic phytoplankton, induced by environmental stimulus, such as cell age, nutrient deprivation, intense light, excessive salt concentrations or oxidative stress (Berman-Frank et al. 2004, Ross 2006, Segovia

2003, Moharikar 2006, Bidle & Bender 2008, Brussaard 1997, Vardi 1999, Bidle 2007). This provides another mechanism by which high lysis rates can be explained independently of viral attack (Bidle et al. 2007). Given its induction by nutrient stresses, PCD was conceptually thought to be a distinct pathway from lytic viral infection. However, studies in *Escherichia coli* and phage T4 have indicated that PCD might also have a role as a virus exclusion defense mechanism to limit multiplication of viruses during infection (Georgiou 1998). Therefore, PCD might be fundamental to prokaryotic and eukaryotic microorganisms with ancient origins.

One of the essential biochemical markers of PCD is the activation of caspase activity. Caspases, or cysteinyl aspartate-specific proteases, have a ubiquitous role in metazoan PCD through the cleavage of various essential proteins (Thornberry 1998). The mechanism by which caspases initiate and execute PCD is through the cleavage of select structures of proteins in a coordinated manner, usually at a single site, resulting in a loss or change in function. (Fischer 2003). Caspases are among the most specific proteases, cleaving at a specific tetrapeptide motif, which differs significantly among caspases and explains the diversity of their biological functions. For example, the tetrapeptide sequence IETD (Ile-Glu-Thr-Asp) corresponds to caspase-8 cleavage specificity; the tetrapeptide sequence YVAD (Tyr-Val-Ala-Asp) corresponds to cleavage specificity of caspase-1 (Thornberry 1997). In laboratory studies, fluorogenic caspase-specific substrates, which contain the canonical tetrapeptide recognition motifs for various caspases bound to a fluorophore via a peptide linkage at aspartate, are

commercially available and commonly used for the direct measurement of caspase activity *in vitro*.

True caspases have only been isolated from multicellular animals but caspase activity has also been reported in vascular plants, yeast (Madeo 2002), trypanosomes (Szallies 2002) and unicellular phytoplankton (Berman-Frank et al. 2004, Ross 2006, Segovia 2003, Moharikar 2006, Bidle & Bender 2008, Brussaard 1997, Vardi 1999, Bidle 2007). At the same time, paracaspases and metacaspases were identified in diverse genome sequences (Uren 2000), including diverse marine phytoplankton (Bidle and Falkowski 2004). Paracaspases and metacaspases share sequence and structural features with caspases and, hence, they are thought to represent ancestral forms of these death-related proteins. Recent findings that they may differ in substrate specificity (Vercammen 2004, Váchová and Palková 2006) suggest that they form distinct families of clan CD cysteine peptidases (Vercammen 2007). Uren (2000) found metacaspases in higher plants, unicellular protists, fungi and specialized bacteria in which metacaspases were required for cell differentiation under nutrient-limiting conditions or different developmental stages. These bacterial species include *Streptomyces*, *Rhizobium*, *Anabaena*, *Bordetella*, *Geosulfurococcus*, *Rhodosphaera*, *Dehalococcoides*, *Xylella* and *Synechocystis* (Uren 2000). This suggests that the genetic signatures of caspase-like genes have been evolving in unicellular organisms for much of earth history, rather than be restricted to the onset of metazoans.

1.2 A role for caspase-like protease in phytoplankton

Analyses of completed genome sequences of prokaryotic and eukaryotic phytoplankton have also revealed the widespread presence of metacaspases (Berman-Frank& Bidle 2004, Wahlund 2004, Venter 2004, Bidle and Falkowski 2004). Phylogenetic analyses using the protein-distance matrix placed phytoplankton metacaspases within the broader context of the caspase family of proteases (Fig 1.2 Bidle and Falkowski 2004). Metacaspase-like proteases from cyanobacteria (colored blue in Fig 1.2) are scattered throughout the phylogenetic tree and form several clusters independent of eukaryotic lineages, suggesting significant lateral gene transfer. In contrast, metacaspases in eukaryotic phytoplankton including red plastid representatives *T. pseudonana* and *E. huxleyi* (Fig 1.2; TpMC and EhMC colored red), and green plastid representative *C. reinhardtii* (Fig 1.2; CrMC colored green) form tight clusters around related organisms, indicative of vertical inheritance. For example, TpMCs and EhMCs cluster within a group of metacaspases that include unicellular protists such as fungi and trypanosomes, while CrMCs cluster strong with metacaspases from higher plants (Fig 1.2 Bidle and Falkowski 2004). Currently, there is no data available on dinoflagellate metacaspases so it is unknown where they cluster within the caspase superfamily.

Recent physiological and biochemical data also indicate that PCD indeed operates in diverse phytoplankton, like cyanobacteria (*Trichodesmium spp., Microcystis aeruginosa*) (Berman-Frank et al. 2004, Ross 2006), chlorophytes (*Dunaliella tertiolecta*, *Chlamydomonas reinhardtii*) (Segovia 2003, Moharikar 2006),

diatoms (*Thalassiosira pseudonana, Ditylum brightwellii)* (Bidle & Bender 2008, Brussaard 1997), dinoflagellate (*Peridinium gatunense*) (Vardi 1999), and coccolithophores (*Emiliania huxleyi)* (Bidle 2007). These organisms showed reduction in biomass and Fv/Fm, morphological degradation of internal components (visualized by transmission electron microscopy), and enhanced cleavage of caspase specific substrates. Furthermore, western blot analyses indicated the induced expression of caspase homologues (Berman-Frank et al. 2004, Segovia 2003, Moharikar 2006, Bidle & Bender 2008, Bidle 2007). For example, antibodies raised against mammalian caspases cross-reacted with specific proteins in *Dunaliella tertiolecta* placed in darkness (Segovia 2003). Antibodies for caspases 1, 3, and 9 cross-reacted with multiple molecular weight bands, whereas antibodies raised against caspases 6 and 8 recognized only one band. Likewise, western blot analyses illustrated immunoreactivity to human caspase-3 polyclonal antisera during *Trichodesmium spp.* bloom progression (Berman-Frank et al. 2004). These results were suggestive of a similar pathway to multicelluar organisms.

Although biochemical and genetic signatures were found in phytoplankton, the relationship between physiology and metacaspase remains to be addressed. With the availability of sequenced genome information, metacaspase gene signatures have been observed in *Thalassiosira pseudonana* (Bidle and Bender 2008), *Emiliania huxleyi* (Bidle 2007), *Micromonas spp.* (Worden 2009), *Aureococcus anophagefferens* (http://genome.jgi-psf.org/Auran1/Auran1.home.html), *Ostreococcus tauri* (Derelle 2006), and *Phaeodactylum tricornutum* (Nedelcu, 2009). With the presence of different

metacaspases in diverse genomes, subsequent efforts have began to specifically look at metacaspase expression in phytoplankton and their potential role in death. The first antibody generated against an *E. huxleyi* metacaspase protein marked a significant transition from focusing on caspases to metacaspases. It still remains the only phytoplankton metacaspase antibody. This polyclonal antibody was generated against an overexpressed and purified, recombinant 36-kDa *E. huxleyi* metacaspase (EhMC) which contained conserved caspase-like domains. The EhMC polyclonal antibody displayed a strong, immuno-hybridization to purified, recombinant human caspase 8, strongly suggesting that metacaspases and caspases shared a similar epitope (Bidle 2007). This antibody was subsequently used to investigate the role of metacaspases in PCD and viral infection in unicellular phytoplankton. Western blot analysis of cell extracts from a sensitive strain *E. huxleyi* 374 infected with virus EhV1 revealed upregulated expression of ~36-kDa and ~42-kDa immunoreactive proteins during viral-induced PCD (Bidle 2007). Strong hybridization of proteins was also observed in the diatom *T. pseudonana* under Fe-stress induced PCD, with proteins ranging in size from ~17 to ~50kDa to the polyclonal EhMC antibody (Bidle and Bender 2008). These data revealed differentially expressed metacaspases between exponentially growing and stressed/dying cells, and suggested that metacaspases are a common, inherent feature whose expression is linked to stress and death. Nonetheless, aside from the aforementioned studies on a coccolithophore (*E.huxleyi*) and a diatom (*T. pseudonana*), very little is known about metacaspase expression in other diverse phytoplankton. Indeed, most metacaspase genes have only been characterized *in silico*. Currently there

is no direct link between phytoplankton metacaspases and caspase activity, cell physiology, raising key questions about their expression and cellular roles.

1.3 Outline of thesis

Fundamental questions remain about the involvement of metacaspases in unicellular lineages of phytoplankton. These include: How widespread is metacaspase expression in diverse phytoplankton? Do diverse phytoplankton express diverse metacaspase homologues? Are metacaspases responsible for observed caspase activities and PCD execution? The major goal of this thesis was to further characterize metacaspase-like protein expression and activity in marine phytoplankton. It specifically combines physiology, biochemistry and proteomics to addresses the following two objectives:

Objective 1: ***Examine metacaspase expression and caspase activity in diverse phytoplankton species under different physiological conditions. (Chapter 2)***

Metacaspase expression and caspase activities were examined in cell cultures of four diverse phytoplankton species, including a chlorophyte (*Dunaliella tertiolecta*), haptophyte (*Isochrysis galbana)*, diatom (*Thalassiosira weissflogii*), and dinoflagellate (*Amphidinium carterae*). These phytoplankton species are representative of different evolutionary lineages of primary, secondary, and tertiary endosymbiotic inheritance. How widespread and how diverse is metacaspase expression and activity? How does

they relate to physiology? Does metacaspase complexity increase with evolutionary complexity?

Objective 2: ***Determine genetic signatures associated with caspase specific activity using a genome enabled approach with the model coccolithophore, E. huxleyi. (Chapter 3)***

An *Ehux1516* and EhV86 host-virus model system was used for sequential purification and characterization of caspase-like proteins, since it was previously shown to dramatically induce caspase specific activity. To date, no gene signatures have been directly linked to observed caspases activities, and this represents a critical gap in our knowledge. The availability of host and viral genomes, as well as model systems to induce caspase activity, allow us to fill this gap. What types of proteins are associated with caspase activity? Based on proteomics data and sequence structure, are they metacaspases or some other yet undefined proteins? Are caspase-like proteases host or viral derived?

Table 1.1 Host range of the *Emiliania huxleyi* virus (EhV) isolates to *E. huxleyi* host strains from the CCMP culture collection (http://ccmp.bigelow.org/) (Table adapted from Schroeder et al. 2002) and comparison of *E. huxleyi* location of isolation.

Virus isolate	*E. huxleyi* host[1]					
	CCMP 370	CCMP 373	CCMP 374	CCMP 379	CCMP 1516	L
*Eh*V84	□	□	+	□	+	+[2]
*Eh*V86	□	□	+	□	+	+[2]
*Eh*V88	□	□	+	□	+	+[2]
*Eh*V163	□	□	+	□	+	+
*Eh*V201	□	□	+	□	+	+
*Eh*V202	□	□	+	□	+	+
*Eh*V203	□	□	+	□	□	+
*Eh*V205	□	□	+	□	+	□
*Eh*V207	□	□	+	□	+	+[2]
*Eh*V208	□	□	+	□	+	+

[1]Culture lysis (+); No evidence of culture lysis (□);
[2]Culture lysis very slow when compared to the other lysed cultures

E. huxleyi strain ID	Location of isolation
CCMP370	North Atlantic, Fjord, Norway
CCMP373	North Atlantic, Sargasso Sea
CCMP374	North Atlantic, Gulf of Maine
CCMP379	North Atlantic, Eddystone, English Channel
CCMP1516	South Pacific

based on information from the Provasoli-Guillard National Center for Culture of Marine Phytoplankton (CCMP); https://ccmp.bigelow.org/

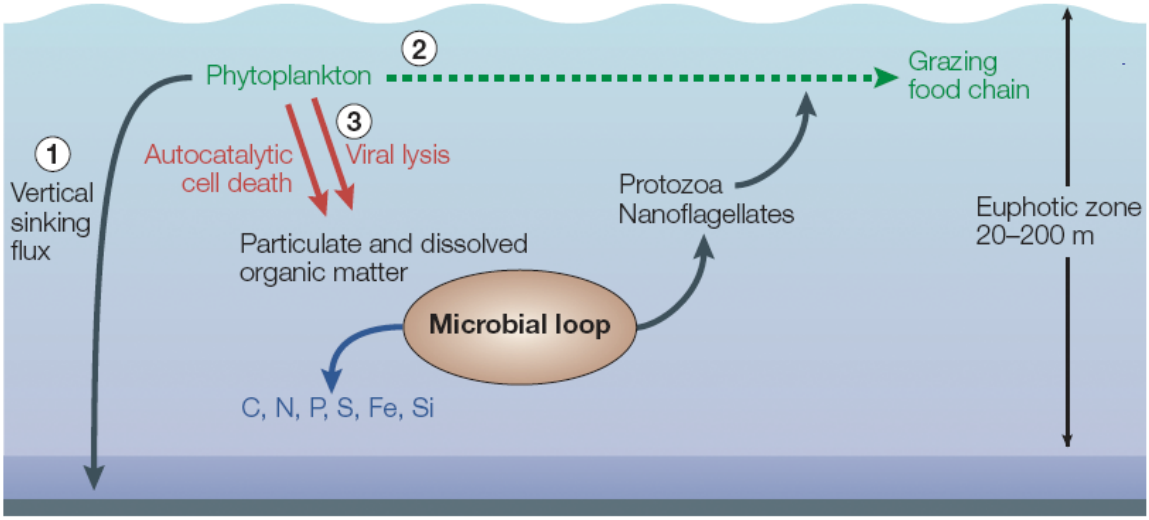

Figure 1.1: A schematic of three major ecosystem pathways in the sea. The important mortality and loss processes independent of grazing (2) and vertical sinking (1) are viral lysis and autocatalytic, programmed cell death (PCD) (3). They help to explain high lysis rates of natural phytoplankton populations and drive globally important biogeochemical cycles in the ocean by channeling organic matter to the microbial loop. (Figure adapted from Bidle and Falkowski 2004)

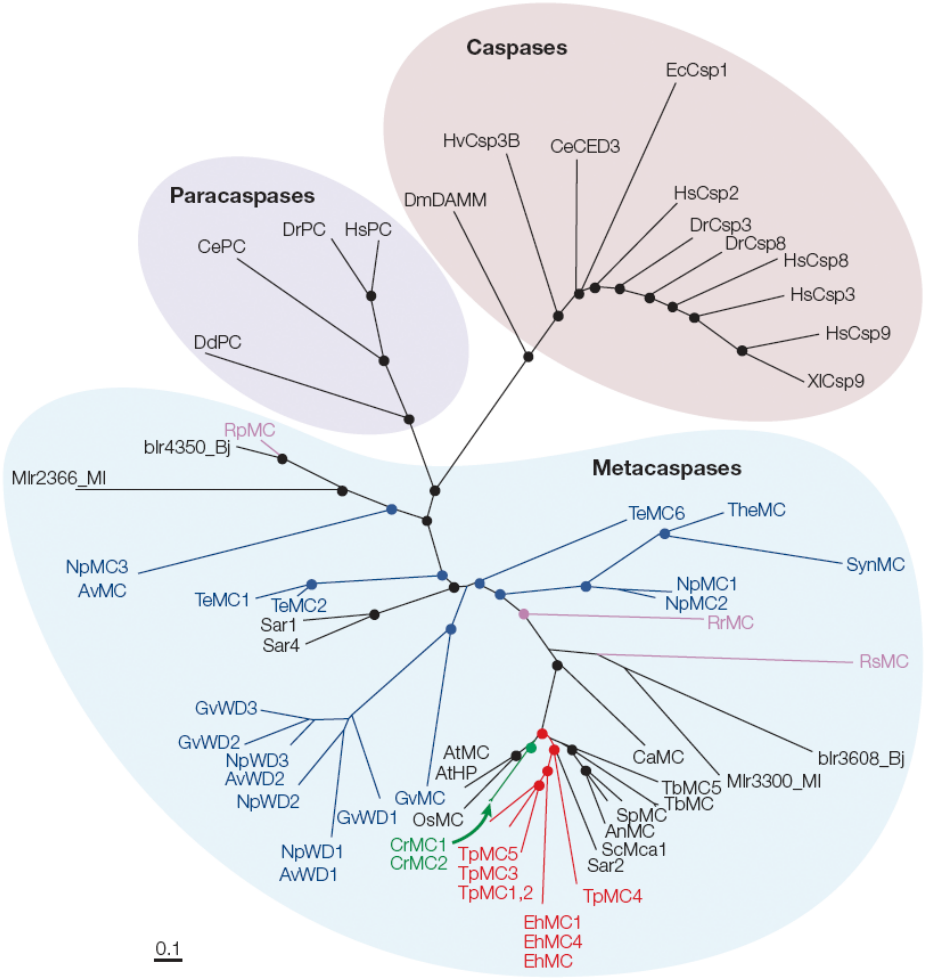

Figure 1.2: Phylogenetic analysis of phytoplankton metacaspases in the larger context of the caspase-family of proteases. Generally, phytoplankton are widely distributed within the metacaspase subgroup. Metacaspases from the 'red' eukaryotic plastid lineages (*T. pseudonana* and *E. huxleyi*; colored red) tightly cluster within a group of metacaspases including unicellular protists such as fungi, and trypanosomes. Metacaspases from 'green' eukaryotic plastid lineages (*C. reinhardtii*; colored green), cluster with higher plants. This is supportive of a vertical line of inheritance. In contrast, metacaspase-like proteases in cyanobacteria (colored blue) show considerable diversity and form several clusters independent of eukaryotic lineages. This suggests considerable lateral gene transfer. Purple non-sulphur photosynthetic bacteria are coloured purple. No metacaspase sequences are available for dinoflagellate, so we are unable to place them on the tree. The scale bar indicates base pair substitutions per nucleotide position. (Figure adapted from Bidle and Falkowski 2004)

Abbreviations:An, *Aspergillus nidulans*; At, *Arabidopsis thaliana*; Av, *Anabaena variabilis*; Bj, *Bradyrhizobium japonicum*; Ca, *Chlorochromatium aggregatum*; Ce, *Caenorhabditis elegans*; Cr, *Chlamydomonas reinhardtii*; Csp, caspase; Dd, *Dictyostelium discoideum*; Dm, *Drosophila melanogaster*; Dr, *Danio rerio*; Eh, *Emiliania huxleyi*; Gv, *Gloeobacter violaceus*; HP, hypothetical protein; Hs, *Homo sapiens*; Hv, *Hydra vulgaris*; MC, metacaspase; Ml, *Mesorhizobium loti*; Np, *Nostoc punctiforme*; Os, *Oryza sativa*; PC, paracaspase; Rp, *Rhodopseudomonas palustris*; Rr, *Rhodospirillum rubrum*; Rs, *Rhodobacter sphaeroides*; Sar, Sargasso Sea; Sc, *Saccharomyces cerevisiae*; Sp, *Schizosaccharomyces pombe*; Syn, *Synechocystis spp.*; Tb, *Trypanosoma brucei*; Te, *Trichodesmium erythraeum*, The, *Thermosynechococcus elongatus*; Tp, *Thalassiosira pseudonana*; WD, WD40-containing protein; Xl, *Xenopus laevis*.

References:

Agustí S. MP Satta, MP Mura, & E Benavent. (1998). Dissolved Esterase Activity as a Tracer of Phytoplankton Lysis: Evidence of High Phytoplankton Lysis Rates in the Northwestern Mediterranean. *LIMNOLOGY AND OCEANOGRAPHY.* **43** (8)**:** 1836-1849.

Azam F. T. Fenchel, et al. (1983). The Ecological Role of Water-Column Microbes in the Sea. *MARINE ECOLOGY PROGRESS SERIES.* **10:** 257-263.

Berman-Frank I. K. D. Bidle, L. Haramaty & P. G. Falkowski. (2004). The Demise of the Marine Cyanobacterium, *Trichodesmium Spp*., Via an Autocatalyzed Cell Death Pathway. *LIMNOLOGY AND OCEANOGRAPHY.* **49** (4)**:** 997-1005.

Bidle K. D. L. Haramaty, J. B. e Ramos, & P. G. Falkowski. (2007). Viral Activation and Recruitment of Metacaspases in the Unicellular Coccolithophore, *Emiliania Huxleyi*. *Proc. Natl. Acad. Sci.* **104** (14)**:** 6049-6054.

Bidle K. D. & P. G. Falkowski. (2004). Cell Death in Planktonic Photosynthetic Microorganisms. *NATURE REVIEWS: MICROBIOLOGY.* **2:** 643-655.

Bidle K. D. & S. J. Bender. (2008). Iron Starvation and Culture Age Activate Metacaspases and Programmed Cell Death in the Marine Diatom *Thalassiosira Pseudonana*. *EUKARYOTIC CELL.* **7** (2)**:** 223-236.

Bratbak G. J. K. Egge, & M. Heldal. (1993). Viral Mortality of the Marine Alga *Emiliania Huxleyi* (Haptophyceae) and Termination of Algal Blooms. *MARINE ECOLOGY PROGRESS SERIES.* **93:** 39-48.

Bratbak G. W. Wilson, & M. Heldal. (1996). Viral Control of *Emiliania Huxleyi* Blooms?. *JOURNAL OF MARINE SYSTEMS.* **9:** 75-81.

Brussaard C. P. D. A. A. M. Noordeloos, & R. Riegman. (1997). Autolysis Kinetics of the W N E Diatom *Ditylum Brightwellii* (Bacillariophyceae) under Nitrogen and Phosphorus Limitation and Starvation. *JOURNAL OF PHYCOLOGY.* **33:** 980-987.

Brussaard C. P. D. R. Riegman *et al.* (1995). Effects of Grazing, Sedimentation and Phytoplankton Cell Lysis on the Structure of a Coastal Pelagic Food Web. *MARINE ECOLOGY PROGRESS SERIES.* **123:** 259-271.

Castberg T. A. Larsen, *et al*. (2001). Microbial Population Dynamics and Diversity During a Bloom of the Marine Coccolithophorid *Emiliania Huxleyi* (Haptophyta). *MARINE ECOLOGY PROGRESS SERIES.* **221:** 39-46.

Cole J. J. S. Findlay, & M. L. Pace. (1988). Bacterial Production in Fresh and Saltwater Ecosystems: A Cross-System Overview. *MARINE ECOLOGY PROGRESS SERIES.* **43:** 1-10.

Cottrell M.T. and C.A. Suttle (1991). Wide-Spread Occurrence and Clonal Variation in Viruses Which Cause Lysis of a Cosmopolitan, Eukaryotic Marine Phytoplankter, *Micromonas Pusilla MARINE ECOLOGY PROGRESS SERIES.* **78:** 1-9.

Derellea E., C. Ferraz, et al. (2006). Genome Analysis of the Smallest Free-Living Eukaryote *Ostreococcus Tauri* Unveils Many Unique Features. *Proc. Natl. Acad. Sci.* **163** (31)**:** 11647-11652.

Field C. B. M. J. Behrenfeld, J. T. Randerson & P. G. Falkowski. (1998). Primary Production of the Biosphere: Integrating Terrestrial and Oceanic Components. *SCIENCE.* **281:** 237-240.

Fischer U. RU Ja¨nicke, & K. Schulze-Osthoff. (2003). Many Cuts to Ruin: A Comprehensive Update of Caspase Substrates. *CELL DEATH AND DIFFERENTIATION.* **10:** 76-100.

Fuhrman. J. A. (1999). Marine Viruses and Their Biogeochemical and Ecological Effects. *NATURE.* **399:** 541-548.

Georgiou T., Y.-T. N. YU, et al. (1998). Specific Peptide-Activated Proteolytic Cleavage of *Escherichia Coli* Elongation Factor Tu. *Proc. Natl. Acad. Sci.* **95:** 2891-2895.

Jacobsen A. G. Bratbak, and M. Heldal. (1996). Isolation and Characterization of a Virus Infecting *Phaeocystis Pouchetii* (Prymnesiophyceae). *JOURNAL OF PHYCOLOGY.* **32** (6)**:** 923 - 927.

Kerr J. F. R. A. H. Wyllie & A. R. Currie. (1972). Apoptosis: A Basic Biological Phenomenon with Wideranging Implications in Tissue Kinetics. *Br. J. CANCER.* **26:** 239-257.

Leist M. & P. Nicotera. (1997). The Shape of Cell Death. *BIOCHEMICAL AND BIOPHYSICAL RESEARCH COMMUNICATIONS.* **236:** 1-9.

Madeo F. E. Herker, *et al*. (2002). A Caspase-Related Protease Regulates Apoptosis in Yeast. *MOLECULAR CELL.* **9:** 911-917.

Mayer J. A. & F. J. R. Taylor. (1979). A Virus Which Lyses the Marine Nanoflagellate *Micromonas Pusilla*. *NATURE.* **281:** 299-301.

Milligan K. L. D. & E. M. Cosper. (1994). Isolation of Virus Capable of Lysing the Brown Tide Microalga, *Aureococcus Anophagefferens*. *SCIENCE.* **266:** 805-807.

Moharikar S. J. S. D'Souza, A. B. Kulkarni, & B. J. Rao. (2006). Apoptotic-Like Cell Death Pathway Is Induced in Unicellular Chlorophyte *Chlamydomonas Reinhardtii* (Chlorophyceae) Cells Following Uv Irradiation: Detection and Functional Analyses. *JOURNAL OF PHYCOLOGY.* **42:** 423-433.

Nagasaki K. & M. Yamaguchi. (1997). Isolation of a Virus Infectious to the Harmful Bloom Causing Microalga *Heterosigma Akashiwo* (Raphidophyceae). *AQUATIC MICROBIAL ECOLOGY.* **13:** 135-140.

Nedelcu. A.M. (2009). Comparative Genomics of Phylogenetically Diverse Unicellular Eukaryotes Provide New Insights into the Genetic Basis for the Evolution of the Programmed Cell Death Machinery. *JOURNAL OF MOLECULAR EVOLUTION.* **68:** 256-268.

Ross C. Lory Santiago-V´azquez, & V. Paul. (2006). Toxin Release in Response to Oxidative Stress and Programmed Cell Death in the

Cyanobacterium *Microcystis Aeruginosa*. *AQUATIC TOXICOLOGY.* **78:** 66-73.

Schroeder D. C. J. Oke, G. Malin, & W. H.Wilson. (2002). Coccolithovirus (*Phycodnaviridae*): Characterisation of a New Large Dsdna Algal Virus That Infects *Emiliania Huxleyi*. *ARCHIVES OF VIROLOGY.* **147:** 1685-1698.

Segovia M. L. Haramaty, J. A. Berges, & P. G. Falkowski. (2003). Cell Death in the Unicellular Chlorophyte *Dunaliella Tertiolecta*. A Hypothesis on the Evolution of Apoptosis in Higher Plants and Metazoans. *PLANT PHYSIOLOGY.* **132:** 99-105.

Suttle C.A. & A. M. Chan. (1995). Viruses Infecting the Marine Prymnesiophyte *Chrysochromulina* Spp.: Isolation, Preliminary Characterization and Natural Abundance. *MARINE ECOLOGY PROGRESS SERIES.* **118:** 275-282.

Szalliesa A. B. K. Kubatac, & M. Duszenkoa. (2002). A Metacaspase of *Trypanosoma Brucei* Causes Loss of Respiration Competence and Clonal Death in the Yeast *Saccharomyces Cerevisiae*. *FEBS LETTERS.* **517:** 144-150.

Thornberry N. A. T. A. Ranol, et al. (1997). A Combinatorial Approach Defines Specificities of Members of the Caspase Family and Granzyme B. *JOURNAL OF BIOLOGICAL CHEMISTRY.* **272** (29)**:** 17907-17911.

Thornberry N. A. & Y. Lazebnik. (1998). Caspases: Enemies Within. *SCIENCE.* **281:** 1312-1316.

Uren A.G. Karen O'Rourke, *et al.* (2000). Identification of Paracaspases and Metacaspases: Two Ancient Families of Caspase-Like Proteins, One of Which Plays a Key Role in Malt Lymphoma,. *MOLECULAR CELL.* **6:** 961-967.

Váchová L., Z. Palková (2006). Caspases in Yeast Apoptosis-like death: Facts and Artefacts. *FEMS Yeast Research.* **7** (1)**:** 12-21.

Van Boekel WHM FC Hansen, R Riegman & RPM Bak. (1992). Lysis-Induced Decline of a *Phaeocystis* Spring Bloom and Coupling with the Microbial Foodweb. *MARINE ECOLOGY PROGRESS SERIES.* **81:** 269-276.

Vardi A. I. Berman-Frank, *et al*. (1999). Programmed Cell Death of the Dinoflagellate *Peridinium Gatunense* Is Mediated by Co2 Limitation and Oxidative Stress. *CURRENT BIOLOGY.* **9:** 1061-1064.

Venter J. C. K. Remington, *et al*. (2004). Environmental Genome Shotgun Sequencing of the Sargasso Sea. *SCIENCE.* **304:** 66-74.

Vercammen D. vdB. Cotte, *et a*l. (2004). Type Ii Metacaspases Atmc4 and Atmc9 of Arabidopsis Thaliana Cleave Substrates after Arginine and Lysine. *JOURNAL OF BIOLOGICAL CHEMISTRY.* **279** (44)**:** 45329-45336.

Vercammen D., W. Declercq, *et al*. (2007). Are Metacaspases Caspases? *JOURNAL OF CELL BIOL.* **179:** 375-380.

Wahlund T. M. A. R. Hadaegh, *et al*. (2004). Analysis of Expressed Sequence Tags from Calcifying Cells of Marine Coccolithophorid (*Emiliania Huxleyi*). *MARINE BIOTECHNOLOGY.* **6:** 278-290.

Walker N. I., B. V. Harmon, G. C Gobé, & J. F. R. Kerr. (1988). In Kinetics and Patterns of Necrosis (Ed. Jasmin, G.) (Karger, Basel, 1988). 18-54.

Wilhelm S.W. & C.A. Suttle (1999). Viruses and Nutrient Cycles in the Sea. *BIOSCIENCE.* **49** (10)**:** 781-788.

Wilson W. H. D. C. Schroeder, *et al*. (2005). Complete Genome Sequence and Lytic Phase Transcription Profile of a *Coccolithovirus*. *SCIENCE.* **309:** 1090-1092.

Wilson W. H. G. A. Tarran, *et al*. (2002). Isolation of Viruses Responsible for the Demise of an *Emiliania Huxleyi* Bloom in the English Channel. *JOURNAL OF THE MARINE BIOLOGICAL ASSOCIATION OF THE UK.* **82** (3)**:** 369-377.

Worden A. Z., J. H. Lee, et al. (2009). Green Evolution and Dynamic Adaptations Revealed by Genomes of the Marine Picoeukaryotes *Micromonas*. *SCIENCE.* **324:** 268-272.

2.0 Metacaspase protein expression and caspase activity in diverse phytoplankton species

2.1 Introduction

Metacaspase gene signatures have been found in diverse phytoplankton, including representatives of prokaryotic cyanobacteria, and derived green and red plastid lineages of eukaryotic phytoplankton (Bidle and Falkowski 2004). The presence of caspase orthologues during death in cyanobacteria (*Trichodesmium spp*.) (Berman-Frank et al. 2004), chlorophyte (*Dunaliella tertiolecta*, *Chlamydomonas reinhardtii*) (Segovia 2003, Moharikar 2006), diatoms (*Thalassiosira pseudonana)* (Bidle & Bender 2008), and coccolithophores (*Emiliania huxleyi)* (Bidle 2007) suggest that phytoplankton have similar PCD execution machinery to metazoans. Along with physiological and morphological characteristics of PCD, these studies have shown the expression of proteins that react with caspase or metacaspases antisera concomitant with elevated caspase specific activity. Importantly, these organisms represent clades that evolved long before the first metazoan (800 Million yr ago), indicating these genes have been established and retained over long evolutionary histories (Bidle and Falkowski 2004).

There is evidence that PCD has a clear mitochondrial connection and bacterial inheritance (Koonin and Aravind 2002). Eukaryotic cell death domains, such

as genes that encode metacaspases, were found in the genomes of the α-Proteobacteria, indicating that they have a bacterial origin, with their subsequent establishment in eukaryotes occurring after a mitochondrial endosymbiotic event and transfer to the nuclear genome. But, given the photosynthetic bacterial (i.e. cyanobacteria) origin of plastids, there is also evidence of plastid role in PCD inheritance. Cyanobacteria are not members of the α-Proteobacteria and gave rise to the chloroplast, not the mitochondrion. Hence, components of the apoptotic machinery in eukaryotic phytoplankton lineages may derive from an endosymbiotic event with a cyanobacterium, and subsequent transfer to the nuclear genome via endosymbiotic gene transfer (Fig 2.1 Bidle and Falkowski 2004).

The evolution of eukaryotic phytoplankton is complicated and has been driven by a variety of endosymbiotic events. Cyanobacteria, also known as blue-green algae, were present in marine ecosystems at least 2.8 Ga based on molecular markers (Summons, 1999) (Fig 2.1) The photosynthetic origins of eukaryotic phytoplankton can be traced to a coccoid cyanobacterium which was phagocytosed by an ancestral, mitochondrion-containing eukaryotic cell and established as an endosymbiont. Many groups of algae have subsequently acquired their plastids via secondary or tertiary endosymbiosis, whereby a photosynthetic eukaryotic cell was itself engulfed by a non-photosynthetic eukaryotic cell (Delwiche 1999). The “green” and “red” eukaryotic plastid lineages are derived from a common plastid type and evolved independently after the primary endosymbiotic event. Most green algae (Chlorophyta), whose plastids are pigmented by chlorophylls *a* and *b*, are of primary endosymbiotic origin. A

different set of green algae possess “secondary” plastids, such as Chlorarachniophyta and the Euglenophyta. Likewise, there are a subset of red algae with primary plastid origin, which are pigmented with chlorophyll *a* and phycobilins and constitute the Rhodophytes. Most of the eukaryotic phytoplankton groups with a red plastid lineage have secondary endosymbiotic origins and these include the cryptomonads (Cryptophyta), the Heterokontophyta (including kelps, diatoms, chrysophytes, and related groups), Haptophyta (the coccolithophorids), and probably those dinoflagellates pigmented with peridinin. Many of these dominate the modern ocean. Tertiary endosymbiotic events are largely restricted to non-photosynthetic dinoflagellate host cells that engulfed diatoms, haptophytes, or cryptophytes, which originated from a secondary endosymbiosis. (Fig 2.2; Delwiche 1999) (Delwiche 1999, Parker 2008).

The fact of marine microalgae derived from primary, secondary, and tertiary endosymbiosis means they have integrated several genomes from the hosts and endosymbionts in order to make a functioning cell. These events have set up an interesting scenario whereby a variety of genetic information has been shared by endosymbiotic gene transfer (EGT), as well as lateral gene transfer (LGT) (Parker 2008). For example, “green gene transfers” constituting 16% of the diatom nuclear coding potential were recently identified using a phylogenomics approach, suggesting an even more complicated diatom history between and green and red eukaryotic lineages (Moustafa, 2009). In addition, numerous genes in diatom genomes were found to be of bacterial origin (Bowler et al. 2009). In turn, these organisms represent a diverse genetic tapestry that influences physiology. We were curious about the

influence of this genetic complexity on the induction and inheritance of PCD in marine phytoplankton. We specifically examined the patterns of metacaspase expression and caspase activities as they relate to cell physiology in four species: a primary derived green lineage chlorophyte (*Dunaliella tertiolecta*), a secondary derived red lineage haptophyte (*Isochrysis galbana*), a distinct secondary derived red lineage diatom (*Thalassiosira weissflogii*), and a tertiary derived red lineage dinoflagellate (*Amphidinium carterae*), all of which do not have whole genome information available. We were especially interested in extending our study to representatives that are often present in natural environments, but do not have sequenced genomes. This allows us to expand our knowledge outside of genetic model systems. Using both cleavage assays of fluorescently labeled caspase-specific substrates and immuno-hybridization to metacaspase antibodies, we address the following questions: Do these diverse phytoplankton display caspase activities? Do they express metacaspase representatives and, if so, how diverse? How does activity and expression relate to physiology and culture dynamics? How does the diversity of metacaspase expression relate to evolutionary complexity?

2.2 Materials and Methods

2.2.1 Culture maintenance and growth conditions

Four species of marine phytoplankton—*Dunaliella tertiolecta* (strain CCMP 1320), *Isochrysis galbana* (strain CCMP 1324), *Thalassiosira weissflogii* (strain CCMP 1336),

and *Amphidinium carterae* (strain CCMP 1314), were batch grown in f/2 medium at 18°C, 14:10 (L:D) cycle with constant aeration. Cell abundance was determined by using a Coulter Multisizer (Beckman Coulter, Fullerton, CA). Fast repetition rate fluorometry (FRRF) was used to derive the maximum photochemical quantum yield of photosystem II (Fv/Fm), an indicator of photosystem health. Cells were pelleted by centrifugation (10,000 g, 4°C, 10 min), frozen in liquid nitrogen, and stored at -80°C until processed.

2.2.2 Detection and measurement of caspase specific activity

Cells were resuspended in caspase activity buffer (Lauber buffer) [(50mM HEPES (pH 7.3)/100 mM NaCl/10% sucrose/0.1% CHAPS/10mM DTT] and sonicated (3*30 sec on ice), and cellular debris was pelleted by centrifugation (14,000 g, 4°C, 5 min). Supernatants were transferred to a fresh tube, incubated with 50μM IETD-AFC (Calbiochem, San Diego, CA) for 4h at 26°C. Fluorescence was measured every 10 mins on a Spectra Max Genimi XS microplate reader using kinetic assay (excitation 400nm, emission 505nm). The BCA assay (Thermo Scientific) was used to determine protein concentration with Bovine Serum Albumin serving as standard. Specific activities were obtained by normalizing hydrolysis rates to total protein.

2.2.3 Western blots analysis

Cell pellets were resuspended in PBS buffer with protease inhibitors [PMSF (0.1mM), Leupeptin (1 μg/ml) and Aprotinin (5 μg/ml)], sonicated (3*30 seconds on ice), and centrifuged (10, 000 g, 4°C, 5 min). Supernatants were transferred to a fresh tube. Equal amount of protein (27μg) were loaded onto 12.5% Tris-HCl SDS/polyacrylamide gels separated by electrophoresis (200V, 1.5h), and transferred onto PVDF membranes (100V, 45 min). Transfer buffer consisted of 3.03g Tris base, 14.4g glycine, and 200mL methanol per liter of MilliQ water. Membranes were probed with polyclonal antisera raised against a purified recombinant *Emiliania huxleyi* metacaspase protein (titer = 1:500) (EhMC; Bidle et al. 2007) followed by polyclonal goat anti-rabbit IgG-HRP (titer = 1:3000), and detected using the Immun-star HRP substrate horseradish peroxidase chemiluminescence system (Bio-Rad).

2.3 Results and discussion

We used batch grown cultures to assess the role of cell physiology on the expression and activity of metacaspases. Given the role of caspase-like proteases in PCD we were particularly interesting in difference between exponential and aging cells of diverse phytoplankton species. Each phytoplankton species we chose (*D. tertiolecta*, *I. galbana, T. weissflogii*, and *A. carterae*) is representative of different evolutionary lineages of primary, secondary, and tertiary endosymbiotic events. The combination of cell abundance data and Fast Repetition Rate Fluorescence (FRRf) data confirmed cell physiology changes for all species during a time course of growth. FRRf has proven

very useful to study changes of phytoplankton physiology as a photosystem health indicator, since it quickly and easily measures the *in vivo* fluorescence signatures of phytoplankton in a non-destructive, non-invasive manner (Kolber 1998).

Each of the four cultures displayed typical batch culture growth dynamics (Fig 2.3). *I. galbana* displayed clearly identifiable lag, exponential, stationary, and death phases. In contrast, *D. tertiolecta*, *T. weissflogii*, and *A. carterae* each showed a long pronounced stationary phase and lacked a dramatic death phase with significant decreases in cell abundance (Fig 2.3). Cell abundance maxima were found to be $3.4*10^6$ ml^{-1} at day 25 (*D. tertiolecta*), $2.0*10^7$ ml^{-1} at day 19 (*I. galbana*), $8.4*10^5$ ml^{-1} at day 11 (*T. weissflogii*), and $8.1*10^5$ ml^{-1} at day 21 (*A. carterae*) (Fig 2.3). During exponential growth, all cultures displayed high Fv/Fm values of 0.4-0.6, characteristic of healthy cells. In contrast, there was a notable and consistent drop in Fv/Fm for each species with transition to stationary phase to 0.1-0.2 in dying cultures.

Measured IETD-AFC hydrolysis rates of cell lysates collected over the time course showed a wide-range of caspase activities among the four species (16 to 391 RFU mg^{-1} h^{-1}). Among the tested species, the highest activity was observed for *A. carterae* on day 23 at 391 RFU mg^{-1} h^{-1}, followed by *I. galbana* on day 23 at 329 RFU mg^{-1} h^{-1}, *T. weissflogii* on day 12 at 234 RFU mg^{-1} h^{-1}. *D. tertiolecta* had the lowest activity on day 25 at 55 RFU mg^{-1} h^{-1} (Fig 2.3). For each individual species, activities generally increased during stationary and death phases. *T. weissflogii* displayed the highest range of caspase activity over the time course, increasing by 12.2 fold. This

was followed by 9.1, 3.8, and 3.4-fold increase in *A. carterae*, *I. galbana* and *D. tertiolecta*, respectively.

Given the affect of compromise physiology on caspase activity, we examined the relationship of caspase activities with specific growth rate (μ) at time of collection. We specifically tested whether these caspase activities were correlated with specific growth rates (Fig 2.4). It has been shown in *Trichodesmium* spp. (Berman-Frank et al. 2004), *T. pseudonana* (Bidle & Bender 2008) and *E. huxleyi* (Bidle et al. 2007) that caspase activity is negatively correlated with specific growth rates. Growth rates were calculated by equation $\mu=[\ln (Nt)-\ln N]/t$ (d^{-1}), with negative growth rate being diagnostic of death phase (= mortality rate). Interestingly, *I. galbana*, had the highest μ (= 1.2 d^{-1}) during exponential phase, but also demonstrated the highest mortality rate (μ = -0.33 d^{-1}), when Fv/Fm decreased down to 0.1. As previously mentioned, most species showed a pronounced stationary phase, which lasted 14 d (*D. tertiolecta*), 7 d (*T. weissflogii*), and 9 d (*A. carterae*), respectively. As a consequence, their mortality rates were lower (*D. tertiolecta*, μ = -0.21 d^{-1}; *T. weissflogii*, μ = -0.07 d^{-1}; *A. carterae*, μ = -0.15 d^{-1}) (Fig 2.3). Specific growth rates generally correlated with caspase activity, although there was considerable variation in the correlation coefficient (R^2). Both *D. tertiolecta* and *T. weissflogii* showed strong correlations with R^2 of 0.58 and 0.99, respectively. In contrast, *I. galbana* and *A. carterae* were only weakly correlated with much lower R^2 of 0.21 and 0.07, respectively. Based on a T-Test analysis, the observed linear regression between caspase specific activity and growth rate was statistically significant for *D. tertiolecta* and *A. carterae* with p-values of

0.050 and 0.0007, respectively. In contrast, the same analysis for *I. galbana* and *T. weissflogii* was not statistically significant with p-values of 0.095 and 0.111, respectively.

At the same time, we examined the pattern of metacaspase expression in these phytoplankton and elucidated its relationship with cell physiology and the observed caspase specific activities. Currently, the EhMC antibody is the only antibody specific for phytoplankton metacaspases. To date this antibody has only been used to assess metacaspase expression in *E. huxleyi* and *T. pseudonana*, both of which have genome sequences and multiple metacaspase genes. In both cases, EhMC immunoreactive proteins correspond to the diversity of annotated putative metacaspases (Bidle and Bender 2008, Bidle et al. 2007). Using Western blot analysis, we tested the utility of the EhMC antibody to assess metacaspase expression diversity in phytoplankton species that don't have sequenced genome data available. Distinct immunoreactive bands were detected for all species tested, suggestive of shared functional epitopes with EhMC (Fig 2.5). Several observations were noteworthy. First, all of the four species revealed constitutive expression of metacaspase-like protein hybridizing to EhMC antibody, indicating EhMC-like proteins are widespread. This suggests a high degree of conservation of caspase-like proteins among phytoplankton species. Similar observations have been seen in *E. huxleyi* and *T. pseudonana*. Importantly, no bands were detected for these species when the membrane was probed with pre-bleed serum, controlling against non-specific signals.

Secondly, the pattern of metacaspase expression was different with species identity. Our observations are consistent with increased metacaspase complexity with evolutionary complexity. The chlorophyte *D. tertiolecta*, representative of a primary endosymbiotic lineage, revealed expression of only one ~20kd protein (Fig 2.5; band 'a'). Interestingly, this resembles the previously published results of *D. tertiolecta* extracts probed with caspase 8 antibody (Segovia 2003). This particular band was slightly upregulated in stationary phase and faded in dying cells. Note that another chlorophyte *Chlamydomonas reinhardtii,* whose genome information is available, has two metacaspase gene sequences (http://genome.jgi-psf.org/Chlre3/Chlre3.home.html). The haptophyte, *I. galbana*, representative of distinct red plastid secondary endosymbiotic lineage, showed downregulated expression of a ~70kD protein (Fig 2.5; band 'b') and a strongly upregulated ~50kD protein (Fig 2.5; band 'c') which was concomitant with elevated caspase activity. The diatom *T. weissflogii*, also representative of a red plastid secondary endosymbiotic lineage, revealed six to seven bands, a notable increase in expression complexity. A ~17 kD protein was slightly upregulated at early time points but subsequently decreased intensity after stationary phase (Fig 2.5; band 'e'), resembling the pattern of a closely related diatom, *T. pseudonana* (Bidle and Bender 2008). Based on genome information, *T. pseudonana* has 6 TpMCs ranging in size from 17-53kD, which are differentially expressed in response to culture age and Fe stress (Bidle & Bender 2008). Lastly, in our tertiary endosymbiotic lineage representative, dinoflagellate *A. carterae* showed the most expressed bands (total bands >7). A ~40kD protein (Fig 2.5; band 'g') was

constitutively expressed in all phases, even during death, and at least 3 proteins (Fig 2.5; band ‘f’, ‘h’, ‘i’) were downregulated at the beginning of death phase.

Although caspase activities generally increased during death phase, metacaspase-like protein expression did not always correlate with elevated caspase activities, which suggests some of the EhMC antibody hybridized proteins are associated with death and caspase-like activity, others may not. It also suggests that the diverse metacaspases may have different physiological roles. Our results add to the ongoing discussion about whether caspase activity and metacaspases are linked. It is still currently unclear whether all metacaspases play a role in executing phytoplankton cell death. For example, it was recently shown that *Aspergillus fumigatus* metacaspases CasA and CasB facilitated growth under physiological stress (Richie 2007), rather than executed cell death. It is noteworthy that two metacaspases in *T. pseudonana* (TpMC5, TpMC6; both with increased transcript abundance in response to Fe limitation) share their best BLAST similarity with *A. fumigatus* CasA (Bidle and Bender 2008). Moreover, cell death in plants, such as tomato (De Jong 2000) and tobacco (del Pozo 1998), has previously been associated with caspase-like activities. However, metacaspases in *Arabidopsis thaliana* have alternative substrate specificity, cleaving after arginine and lysine rather than aspartate, indicating some types of metacaspase are not directly responsible for reported caspase-like activities in plants (Vercammen et al. 2004). This raises the question as to whether metacaspases confer caspase activity and directly leads to our next objective of linking observed caspase activities with genetic signatures in unicellular phytoplankton.

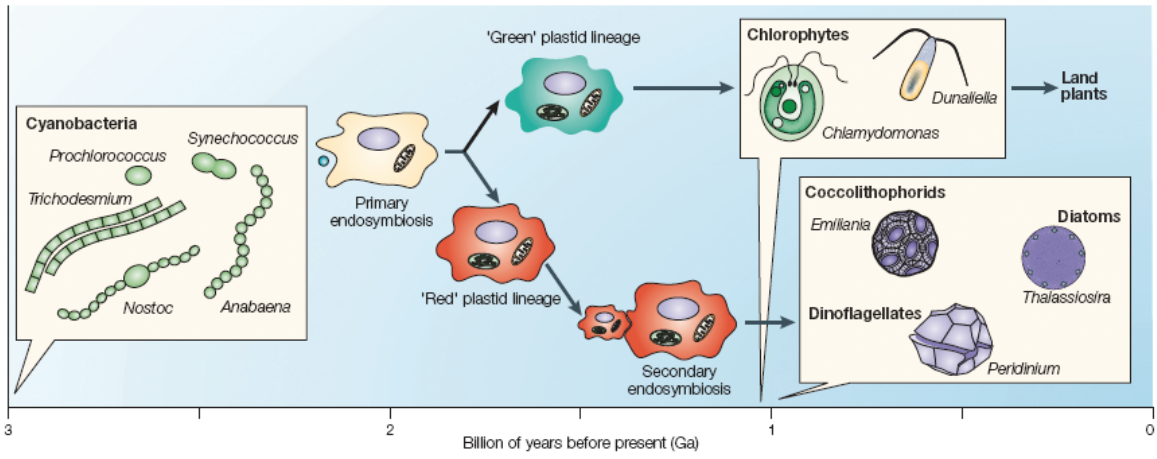

Figure 2.1: Evolutionary context of major marine phytoplankton groups, in relation to the endosymbiotic events. Most phytoplankton in the contemporary ocean are cyanobacteria, which, based on the presence of molecular markers, were present in marine ecosystems at least 2.8 billion years ago (Ga). The chlorophytes (eg, *Dunaliella*) are members of the green lineage which eventually gave rise to land plants ~0.45 Ga. The red lineage includes diatoms (eg, *Thalassiosira*), haptophytes (eg, *Emiliania*, *Isochrysis*) and dinoflagellates (eg, *Amphidinium*), has come to dominate the modern ocean. Physiological, biochemical and genetic evidence of PCD markers in cyanobacteria and derived eukaryotic lineages suggest apoptosis has deep evolutionary roots. The apoptotic machinery in eukaryotic phytoplankton lineages may have been established by an endosymbiotic event with a cyanobacterium, retained in independently evolving superfamilies and subsequently transferred to the nuclear genome of the host. The cyanobacteria have considerable diversity in the phylogenetic analysis of the caspase-like protein family, forming several distinct clusters. (Figure adapted from Bidle and Falkowski 2004)

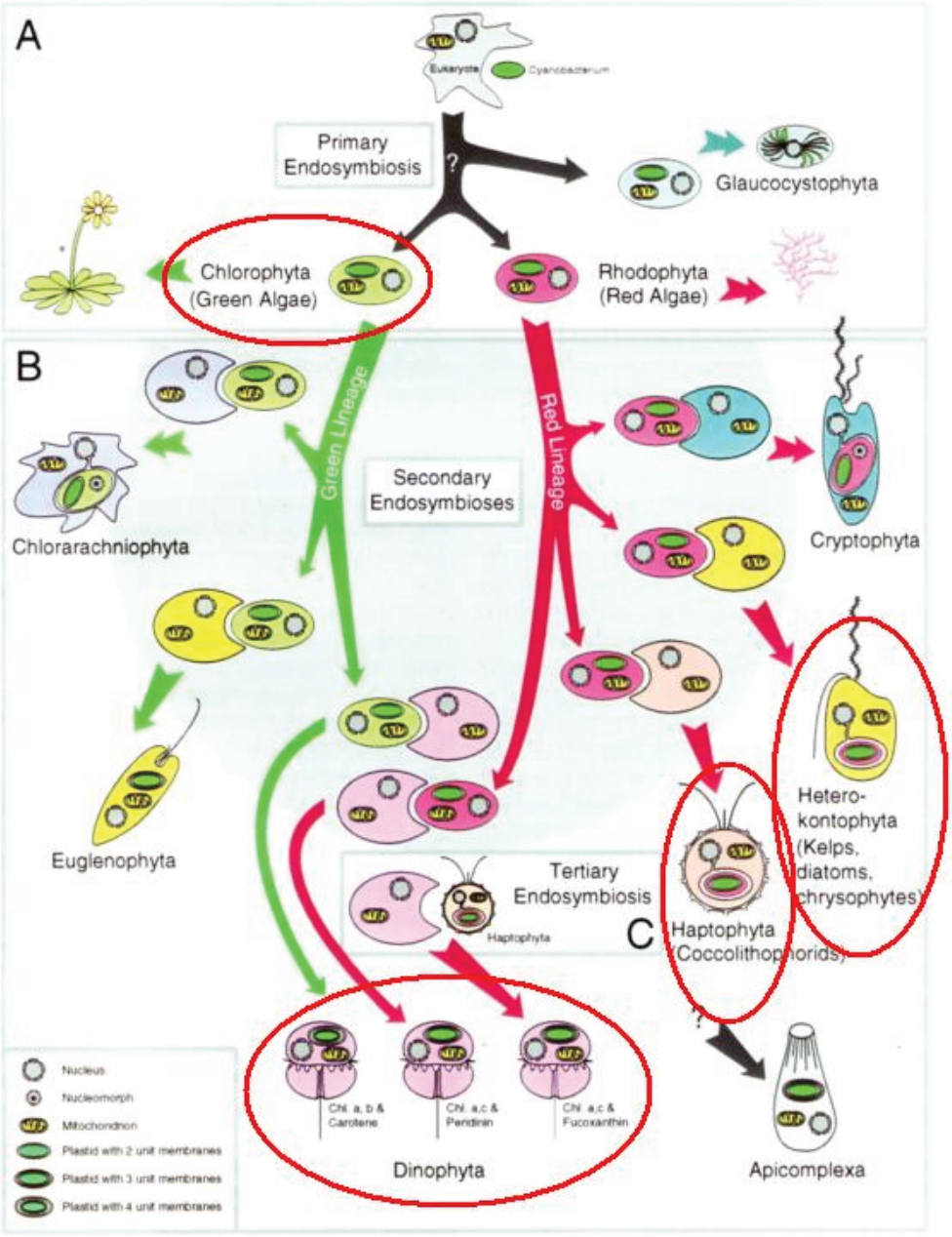

Figure 2.2: Evolutionary history of eukaryotic phytoplankton showing the endosymbiotic events and the development of plastid lineages. Phytoplankton evolution spans both bacterial and eukaryotic domains of life and at least eight major eukaryotic divisions or phyla. The photosynthetic origins eukaryotic phytoplankton can be traced to an endosymbiotic event between an ancestral, mitochondrion-containing eukaryotic cell and a coccoid cyanobacterium. A) Three algal lineages with primary plastids can be identified, each marked by its distinctive plastid type: the red algae (Rhodophyta), green algae (Chlorophyta), and Glaucocystophyta. B) Two ancient superfamilies, the green and red lineages, evolved independently after the primary endosymbiotic event. A number of secondary endosymbiotic events resulted in the acquisition of plastids via predation of a plastid-containing eukaryote by a second eukaryote. The organisms in our study are from four distinct major phyla (red circles) and represented primary, secondary and tertiary lineages. (Figure adapted from Delwiche 1999)

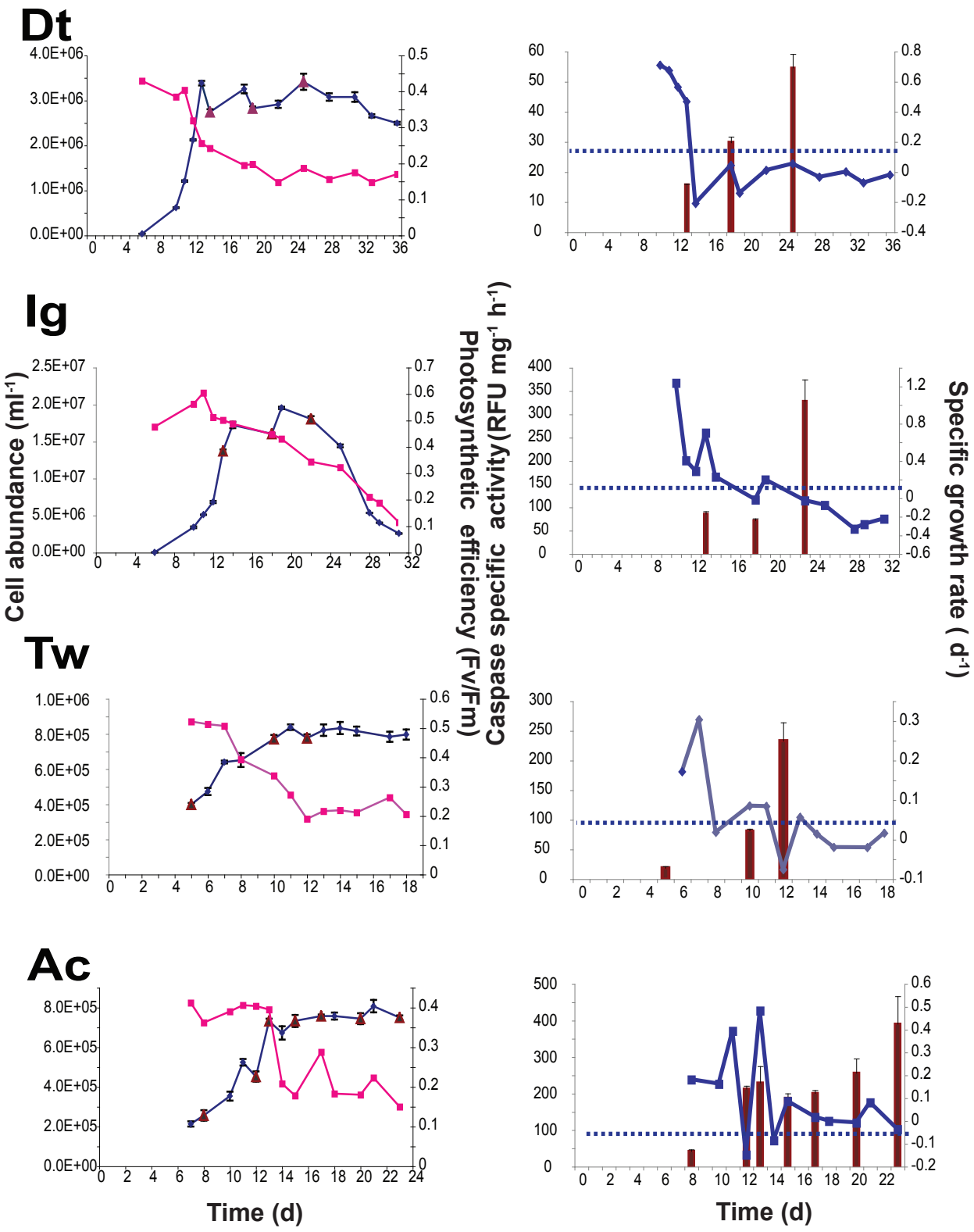

Figure 2.3: Time course of cell dynamics for four phytoplankton species growing in replete culture media. Left panel: cell abundance (blue lines) and photosynthetic efficiency (purple lines); Right panel: growth rate (blue lines) and caspase specific activity (red columns). *Dunaliella tertiolecta* (Dt), *Isochrysis galbana* (Ig), *Thalassiosira weissflogii* (Tw), and *Amphidinium carterae* (Ac) incubating in f/2 batch culture at 18°C, under 14:10 light: dark cycle and constant bubbling. Dark red symbols on growth curves represent times where cell pellets were harvest for activity assays and Western blots analysis. Error bars represent standard deviation from triplicate measurements. Dotted lines represent growth rate 0.

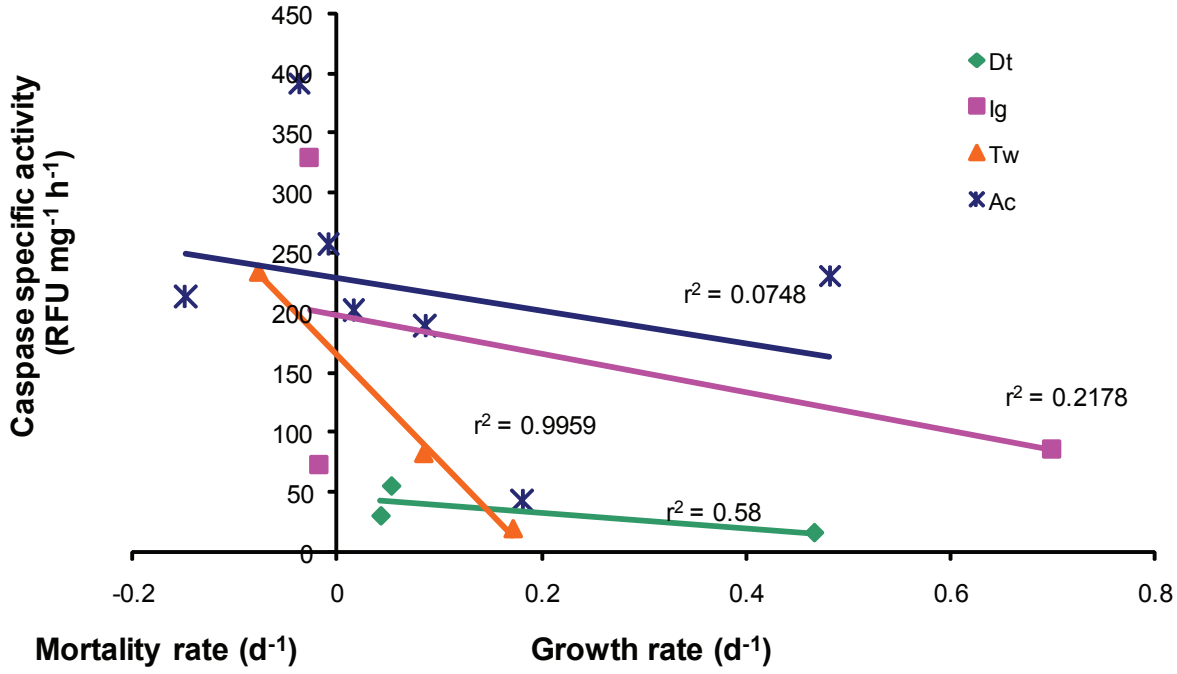

Figure 2.4: Relationship between caspase activity and specific growth rate for the four phytoplankton species. Linear regressions were performed with the indicated correlation coefficients. Green; *D. tertiolecta* (y = -61.908x + 45.124); Purple; *I. galbana* (y = -161.59x + 198.03); Orange; *T. weissflogii* (y = -874.41x + 163.92); Blue; *A. carterae* (y = -137.75x + 229.23).

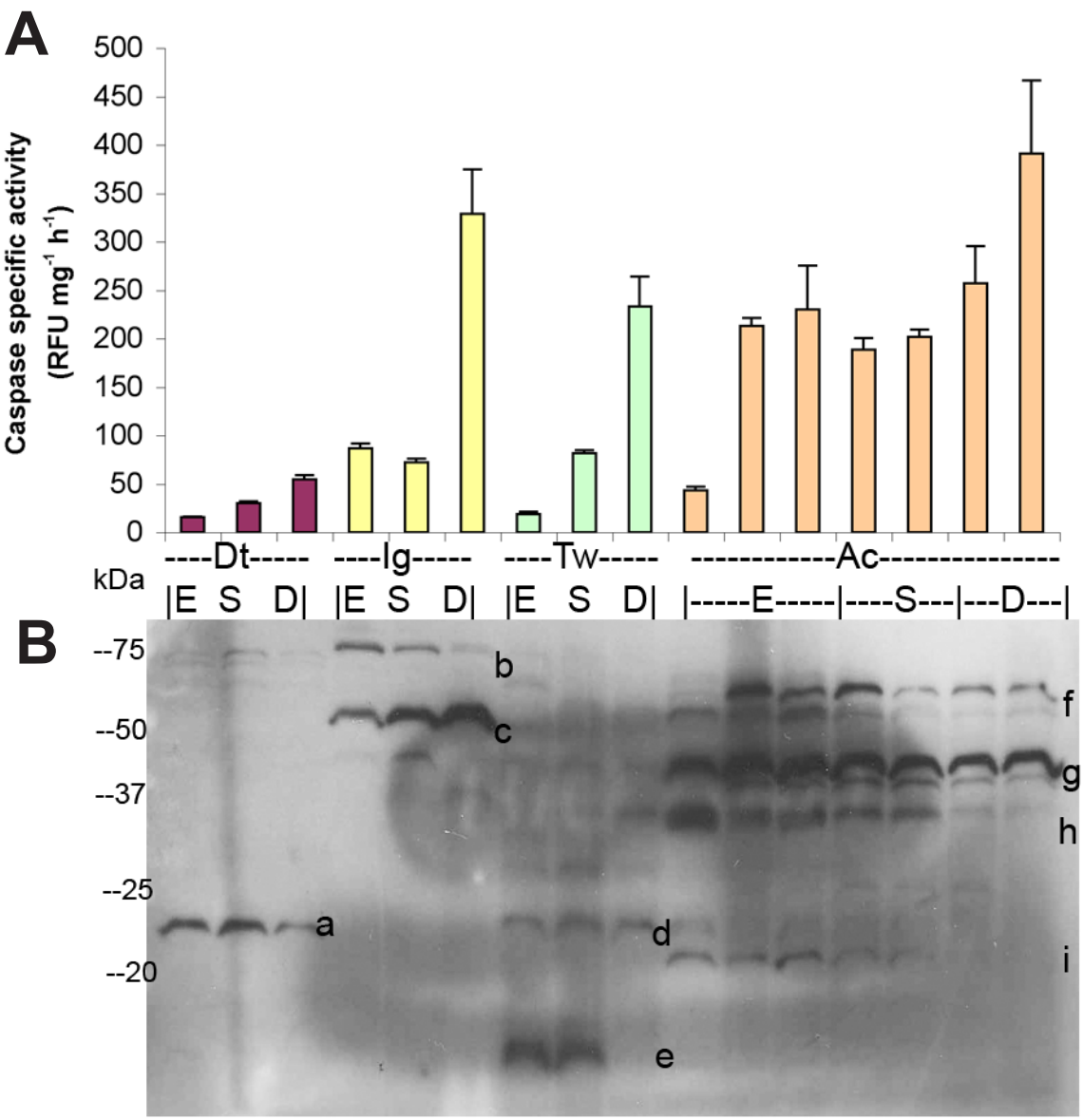

Figure 2.5: Caspase specific activity (A) and metacaspase protein expression (B) of the four phytoplankton species at different phases of growth. (Dt, *Dunaliella tertiolecta*; Ig, *Isochrysis galbana*; Tw, *Thalassiosira weissflogii*; Ac, *Amphidinium carterae*; E, exponential; S, stationary; D, death.) Death phases were defined by negative specific growth rate μ, d^{-1}. In (A), biochemical analysis of cell lysates collected over the time course showed a wide-range of specific caspase activities from 16 to 391 RFU mg^{-1} h^{-1}. Activities generally increased during death phase. In (B), a polyclonal EhMC antibody was used to investigate metacaspase protein expression. Western blot analysis detected distinct bands for all species tested, some of which persisted during death.

References:

Berman-Frank I. K. D. Bidle, L. Haramaty & P. G. Falkowski. (2004). The Demise of the Marine Cyanobacterium, *Trichodesmium Spp*., Via an Autocatalyzed Cell Death Pathway. *LIMNOLOGY AND OCEANOGRAPHY.* **49** (4)**:** 997-1005.

Bidle K. D. L. Haramaty, J. B. e Ramos, & P. G. Falkowski. (2007). Viral Activation and Recruitment of Metacaspases in the Unicellular Coccolithophore, *Emiliania Huxleyi*. *Proc. Natl. Acad. Sci.* **104** (14)**:** 6049-6054.

Bidle K. D. & P. G. Falkowski. (2004). Cell Death in Planktonic Photosynthetic Microorganisms. *NATURE REVIEWS: MICROBIOLOGY.* **2:** 643-655.

Bidle K. D. & S. J. Bender. (2008). Iron Starvation and Culture Age Activate Metacaspases and Programmed Cell Death in the Marine Diatom *Thalassiosira Pseudonana*. *EUKARYOTIC CELL.* **7** (2)**:** 223-236.

Bowler C., A. E. Allen, et al. (2008). The *Phaeodactylum* Genome Reveals the Evolutionary History of Diatom Genomes. *NATURE.* **456:** 239-244.

De Jong A. J., F. A. Hoeberichts, et al. (2000). Chemical-Induced Apoptotic Cell Death in Tomato Cells: Involvement of Caspase-Like Proteases. *PLANTA.* **211:** 656-662.

del Pozo O. & E. Lam (1998). Caspases and Programmed Cell Death in the Hypersensitive Response of Plants to Pathogens. *CURRENT BIOLOGY.* **8** (20)**:** 1129-1132.

Delwiche. C. F. (1999). Tracing the Thread of Plastid Diversity through the Tapestry of Life. *THE AMERICAN NATURALIST.* **154:** S164-S177.

Kolber Z. S. O.Pra¨sil, & P. G. Falkowski. (1998). Measurements of Variable Chlorophyll Fluorescence Using Fast Repetition Rate Techniques: Defining Methodology and Experimental Protocols. *BIOCHIMICA ET BIOPHYSICA ACTA.* **1367:** 88-106.

Koonin E.V. & L. Aravind. (2002). Origin and Evolution of Eukaryotic Apoptosis: The Bacterial Connection. *CELL DEATH AND DIFFERENTIATION.* **9:** 394-404.

Moharikar S. J. S. D'Souza, A. B. Kulkarni, & B. J. Rao. (2006). Apoptotic-Like Cell Death Pathway Is Induced in Unicellular Chlorophyte *Chlamydomonas Reinhardtii* (Chlorophyceae) Cells Following Uv Irradiation: Detection and Functional Analyses. *JOURNAL OF PHYCOLOGY.* **42:** 423-433.

Moustafa A., B. Beszteri, et al. (2009). Genomic Footprints of a Cryptic Plastid Endosymbiosis in Diatoms. *SCIENCE.* **324:** 1724-1726.

Parker M. S., T. Mock, & E. V. Armbrust. (2008). Genomic Insights into Marine Microalgae. *ANNUAL REVIEW OF GENETICS.* **42:** 619-645.

Richie D. L., M. D. Miley, et al. (2007). The *Aspergillus Fumigatus* Metacaspases Casa and Casb Facilitate Growth under Conditions of Endoplasmic Reticulum Stress. *MOLECULAR MICROBIOLOGY.* **63** (2)**:** 591-604.

Segovia M. L. Haramaty, J. A. Berges, & P. G. Falkowski. (2003). Cell Death in the Unicellular Chlorophyte *Dunaliella Tertiolecta*. A Hypothesis on the Evolution of Apoptosis in Higher Plants and Metazoans. *PLANT PHYSIOLOGY.* **132:** 99-105.

Summons R. E L. L. Jahnke, J. M. Hope & G. A. Logan. (1999). 2-Methylhopanoids as Biomarkers for Cyanobacterial Oxygenic Photosynthesis. *NATURE.* **400:** 554-557.

Vercammen D. vdB. Cotte, et al. (2004). Type Ii Metacaspases Atmc4 and Atmc9 of *Arabidopsis Thaliana* Cleave Substrates after Arginine and Lysine. *JOURNAL OF BIOLOGICAL CHEMISTRY.* **279** (44)**:** 45329-45336.

3.0 Purification and characterization of caspase activity-associated proteins in the coccolithophore, *Emiliania huxleyi*

3.1 Introduction

Caspase activities are widespread in plants and unicellular protists, including phytoplankton, yeast, and trypanosomes, (Madeo 2002, Szallies 2002, Bidle & Falkowski 2004), yet there is a general lack of consensus as to whether metacaspases are responsible for the observed caspase activities in these organisms. Indeed, while metacaspases in yeast and trypanosomes have been shown to have caspase activity (Madeo 2002, Szallies 2002), in other systems (e.g., plants), metacaspases have altered substrate specificities indicating they may not be directly responsible for caspase-like activity (Vercammen et al. 2004). Currently, there is no direct link between caspase specific activity and metacaspases in phytoplankton, and this is a fundamental gap in our knowledge about these enzymes. Before we can understand how PCD-genes evolved in phytoplankton, we need to ascribe genetic signatures to key diagnostic activities, like caspase specific activities. Are metacaspases associated with observed caspase activities? If not, what other unknown enzymes are responsible?

We took a genome-enabled protein biochemistry and proteomics approach to address this issue. Our specific goal was to identify proteins that may be

responsible for observed caspase activity. We used an *E. huxleyi* CCMP 1516 (*Ehux1516)* and *E. huxleyi* virus 86 (EhV86), the type-strain for the giant double-stranded DNA coccolithoviruses, host-virus system as model system to approach this objective. *E. huxleyi* (Prymnesiophyte, Haptophyceae) belongs to the coccolithophores, a class of unicellular phytoplankton with chlorophyte lineage that often dominates phytoplankton blooms in the modern ocean and plays an important role in the carbon cycle, through photosynthesis and precipitation of calcium carbonate. It is often infected by virus or virus-like particles, both sensitive strains and resistant strain were studied in the field and laboratory (Table 3.1 Schroeder 2002).

It is known that viral gene products induce caspase-mediated apoptosis in animals (Teodoro 1997), suggesting that viruses have evolved a physiological relationship with PCD. As a member of the family of nucleocytoplasmic large DNA viruses (NCLDV), EhV86 has the capacity to transcribe its genome (Allen 2006), including virally encoded glycosphingolipids that induce PCD (Vardi 2009), as a strategy to synthesize virions in the cytoplasm. Indeed, PCD markers were observed in the Ehux-EhV system, such that sensitive strain *Ehux374* showed strong activation of caspase activity and recruitment of metacaspases of the PCD pathway (Bidle et al. 2007). The biochemical interaction between *E. huxleyi* 374 and EhV1 consisted of an up-regulation of metacaspase protein expression, and massive induction of caspase-like activity, concomitant with the lytic phase of infection (Bidle et al. 2007).

Based on these observations that viral infection of *E. huxleyi* induces PCD and caspase activity, we extend our investigations to a different host (*Ehux1516*) and virus (EhV86) strains, with available genetic information. The *Ehux1516* genome has been sequenced, with nearly complete annotation (http://genome.jgi-psf.org/Emihu1/Emihu1.home.html) and the genome sequence of EhV86 was recently reported (Wilson 2005). The fact that *Ehux1516* and EhV86 genomes have been sequenced allows us to identify proteins associated with strongly induced caspase activities and to test the hypothesis that viral gene products may be responsible for this activity.

3.2 Materials and Methods

3.2.1 Growth and Monitoring of *Emiliania huxleyi*

Emiliania huxleyi strain CCMP 1516 was grown in batch culture in f/2 medium at 18°C, 14:10 (L:D) cycle with constant aeration. Cell abundance was determined by using a Coulter Multisizer (Beckman Coulter, Fullerton, CA). Fast repetition rate fluorometry (FRRF) was used to derive the maximum photochemical quantum yield of photosystem II (Fv/Fm), an indicator of photosystem health. Cells were pelleted by centrifugation (10,000 g, 4°C, 10 min), frozen in liquid nitrogen, and stored at -80°C until processed.

3.2.2 Viral Infection

An active viral stock of EhV86, was propagated by infecting batch cultures of *Ehux1516* grown in f/2 (minus Si). For the experimental set up, a 8 L *Ehux1516* culture was grown to a cell density of ~1.5×10^6 cells per ml and subsequently split into two equal components (4 L each), one representing a virus-free control and the other infected with EhV86 at 20:1 host: virus (V:V). Infection was monitored by measuring host cell abundance and Fv/Fm, as well as viral abundance (as described in Bidle et al. 2007). Viral lysates were centrifuged (10,000 g, 4°C, 10 min) and passed through 0.4-μm polycarbonate syringe filters to remove cellular and particulate debris. SYBR green, a fluorescent DNA intercalating stain, was used to count virus particles via epifluorescence microscopy (Bidle et al. 2007).

3.2.3 Detection and measurement of caspase specific activity

Cells were resuspended in caspase activity buffer (Lauber buffer) [(50mM HEPES (pH 7.3)/100 mM NaCl/10% sucrose/0.1% CHAPS/10mM DTT] and sonicated (3*30 sec on ice), and cellular debris was pelleted by centrifugation (14,000 g, 4°C, 5 min). Supernatants were transferred to a fresh tube, incubated with 50μM IETD-AFC or YVAD-AFC (Calbiochem, San Diego, CA) for 4h at 26°C. Fluorescence was measured every 10 mins on a Spectra Max Genimi XS microplate reader using kinetic assay (excitation 400nm, emission 505nm). The BCA assay (Thermo Scientific) was used to determine protein concentration with Bovine Serum Albumin serving as

standard. Specific activities were obtained by normalizing hydrolysis rates to total protein.

3.2.4 Western blots analysis

Cell pellets were resuspended in PBS buffer with protease inhibitors [PMSF (0.1mM), Leupeptin (1 μg/ml) and Aprotinin (5 μg/ml)], sonicated (3*30 seconds on ice), and centrifuged (10, 000 g, 4°C, 5 min). Supernatants were transferred to a fresh tube. Equal amount of protein (10.5μg) were loaded onto 10% Tris-HCl SDS/polyacrylamide gels, separated by electrophoresis (150V, 1.5h), and transferred onto PVDF membranes (100V, 45 min). Transfer buffer consisted of 3.03g Tris base, 14.4g glycine, and 200mL methanol per liter of MilliQ water. Membranes were probed with polyclonal antisera raised against a purified recombinant *Emiliania huxleyi* metacaspase protein (titer = 1:500) (EhMC; Bidle et al. 2007) followed by polyclonal goat anti-rabbit IgG-HRP (titer = 1:3000), and detected using the Immun-star HRP substrate horseradish peroxidase chemiluminescence system (Bio-Rad).

3.2.5 Protein Purification

Assay of Protease Inhibitors. Four protease inhibitors: EDTA (0.2mM), PMSF (0.2mM), Leupeptin (1 μg/ml) and Aprotinin (5 μg/ml), were added to the cell extracts individually to test for potential caspase inhibition and compatibility with YVAD-AFC hydrolysis assay. Samples were also treated with a mixture of PMSF, Leupeptin and

Aprotinin. After addition of the protease inhibitor, extracts were incubated for 5 minutes prior to the addition of YVAD-AFC substrate, and measurement of hydrolysis activity via the aforementioned fluorescence assay. An incubation time of 24 hours was also tested.

Ammonium Sulfate Precipitation. Cell pellets were resuspended in 5ml PBS buffer and sonicated (3*30 seconds on ice). Cell extracts were clarified by centrifugation (10,000 g, 4°C, 5 min). A small aliquot (0.3ml) was removed prior to precipitation for comparison and represented total activity. For optimal stirring and homogeneity, a 30ml solution volume was used by adding 0.22μm filtered PBS. Fractions were successively precipitated at ammonium sulfate ($AmSO_4$) saturations of 25, 50, 70, and 90% (Englard and Seifter 1990). Ammonium sulfate was added in increments with constant stirring. Precipitated proteins were removed at each step by centrifugation (10,000g, 4°C, 10 min). The individual precipitates were dissolved in <1ml of 0.22μm filtered PBS. Removal of ammonium sulfate of 50, 70 and 90% fractions was accomplished by dialysis at 0-4°C in PBS buffer overnight. Protein concentration (BCA assay) and caspase specific activity (YVAD-AFC substrate) were performed for all fractions, as previously described.

Ion Exchange Chromatography. Ion exchange chromatography (IEC) was employed using solid-phase packing of Bio-Scale Mini Macro-Prep High Q anion exchange 1ml Cartridge. Due to its optimal caspase specific activity, the 70% $AmSO_4$ fraction was selected for further separation via IEC. Samples were loaded onto the

column using a syringe and a flow rate 2.0 ml/min was maintained. Tris-HCl buffer (100mM, pH7.4) was used as the elution buffer with an increasing NaCl discontinuous step gradient of 150mM, 250mM, 500mM, 750mM, 1M, 1.5M and 2M. Protein concentration (BCA assay) and caspase specific activity (YVAD-AFC substrate) were performed for all fractions, as previously described.

Size Exclusion Chromatography. Size Exclusion Chromatography (SEC) (BioRad P-100 gel filtration column) was performed for further separation of IEC fractions. A flow rate of 4.0cm hr^{-1} was maintained by gravity. Molecular weight calibration mixtures (BioRad gel filtration standards) were used to identify proteins of known molecular weight and calibrate the column separation resolution. The UV absorption at 280nnm (A280) was used to estimate protein concentration. Caspase specific activity (YVAD-AFC substrate) was performed for all fractions, as previously described.

Dot Blot Analysis. Either equal amounts of proteins or equal caspase activity from each fraction was pipetted onto a nitrocellulose membrane, using a microfiltration blotting system (Bio-Rad), and the membrane was allowed to air dry. When dry, the membrane was incubated in blocking solution (5% milk) for 1 hour. After incubation, membranes were then probed with polyclonal antisera raised against a purified recombinant *Emiliania huxleyi* metacaspase protein (titer = 1:500) (EhMC; Bidle et al. 2007) followed by polyclonal goat anti-rabbit IgG-HRP (titer = 1:3000), and detected

using the Immun-star HRP substrate horseradish peroxidase chemiluminescence system (Bio-Rad).

3.2.6 Protein mass spectrometry

SEC purified fractions that possessed the highest caspase specific activities were subjected to denaturing SDS-PAGE and mass spectrometry analysis. The Thermo Scientific Pierce Silver Stain Kit (also called SilverSNAP Silver Stain Kit II), a sensitive and reliable mass spectrometry compatible silver stain, was used to visualize protein bands, according to manufacturer's instructions. This stain allows visualization of bands down to 5ng. After silver staining the gel according to manufacturer's protocols, bands of interest were excised using a clean scalpel.

Excised samples were submitted to the Center for Advanced Biotechnology and Medicine (CABM) for mass spectrometry analysis. The CABM and Robert Wood Johnson Medical School, both on the Busch campus of Rutgers University, co-operate a Biological Mass Spectrometry Facility. This facility is equipped with LC-MS/MS (Thermo LTQ and Dionex U-3000) and Applied Biosystems ABI-MDS SCIEX 4800MALDI-TOF/TOF and Voyager DE-PRO mass spectrometers. Output RAW files were analyzed using GPM X! Tandem Spectrum Modeler (http://thegpm.org/map/gpmo_system.html). Output peptide fragments were searched against the following web-based sequence databases: Emihu1_reduced_proteins.fasta.gz, Emihu1_best_proteins.fasta.gz, and

Emihu1_all_proteins.fasta.gz from the *E. huxleyi CCMP1516* genome sequencing project. The *E. huxleyi* sequence data was produced by the US Department of Energy Joint Genome Institute (http://www.jgi.doe.gov/) in collaboration with the user community.

Additional active SEC fractions were sent to Medical University of South Carolina (MUSC) for 2D gel electrophoresis (GE) and proteomic analysis. Fraction samples included: pooled subsets of caspase active fractions, a pooled subset of non-active fraction (negative control), and a 6x His-tagged purified, recombinant *E. huxleyi* metacaspase (EhMC; Protein ID 440238; positive control). At MUSC, proteins were first precipitated using TCA/ACETONE to remove salts, and then resuspended in buffer compatible with 2D-DIGE (two dimensional differential gel electrophoresis). Concentrations were determined by Bradford method. Depending upon the quantity of protein available, 1-10 μg was used per 2D gel and run using 3-10 IPG strips in the first dimension and SDS-PAGE (4-12% 11cm) in second dimension. Gels were stained with Sypro Ruby to visualize spots. Spots were cut and digested with trypsin. All spots within the range that exceed an intensity threshold for successful identification were picked for MALDI-TOF-TOF (MASCOT). Peptides were purified using ZIP TIPS (c18) and spotted onto MALDI targets for TOF-TOF analysis Peptides were searched against the web-based sequence databases from the *E. huxleyi CCMP1516* genome sequencing project (list above). They were also searched against a forward and randomized protein library to assess a threshold for false discoveries.

3.3 Results and discussion

We observed successful infection of *Ehux1516* with EhV86 (Fig 3.1 a), with ~75% reduction in cell abundance within 180 hrs (Fig 3.1 b). EhV86 infection significantly impaired the maximum photochemical quantum yield of photosystem II (Fv/Fm), which declined by 40% after 120 h. Fv/Fm values were decoupled from virus infection at later time points, as control and virus infection were similar (Fig. 3.1c). The infected *Ehux1516* culture was terminated after the 276-h viral time course. Control cultures showed no signs of clearing within this time period (Fig 3.1a & b). Virus abundance peaked at day 10 with 3.9×10^7 viruses ml^{-1}, which corresponded to a burst size ~10 (Fig 3.1 b). Our observed host-virus dynamics differed from a previous study, whereby infection of another sensitive strain *Ehux374* with EhV1 was complete after a 60-h viral time course and resulted in ~90% reduction in cell abundance, with viral abundances peaking in excess of 3×10^9 ml^{-1}. This corresponded to a mature burst size of 800 viruses per cell (Bidle et al. 2007). The differences in viral-host dynamics between our virus-host system is likely due to both host and virus strain specific properties.

We verified that caspase-like proteases were induced during viral infection and cell death by *in vitro* measurements of enzymatic cleavage of the fluorogenic, caspase-specific tetrapeptide substrates IETD-AFC (Ile-Glu-Thr-Asp-AFC) and YVAD-AFC (Tyr-Val-Ala-Asp-AFC), which correspond to caspase 8 and caspase 1, respectively. These substrates have shown to be the most effective with *E. huxleyi* extracts (this study). EhV86 infection of *Ehux1516* triggered as much as 143-fold and

172-fold increase in caspase specific activity in cell extracts, as assessed via cleavage of IETD-AFC and YVAD-AFC, respectively (Fig 3.2). These values closely compared to a ~200-fold increase in caspase specific activity *via* IETD-AFC cleavage during EhV1 infection of *Ehux374* (Bidle et al. 2007). In our study, caspase specific activity generally peaked during the late phase (>120h) of lytic cycle (Fig 3.2), whereas uninfected control cultures displayed <1% of this peak activity. Interestingly, caspase specific activities as measured by YVAD-AFC cleavage were at least twice that obtained by IETD-AFC cleavage in all samples. For example, at 276 hours post infection, specific activity was 9734 RFU mg^{-1} h^{-1} and 5135 RFU mg^{-1} h^{-1}, respectively (Fig 3.2).

Western blot analysis of cell extracts probed with an EhMC polyclonal antisera revealed dynamic expression of ~50-kDa and ~36-kDa metacaspase-like proteins in EhV86 infected *Ehux1516* cells during a 13 day time course (Fig. 3.3 b). The ~36 kDa protein was strongly expressed at early time points (0-192 h) but disappeared after 240 h. Notably, EhV86 infection post 240 h triggered the strong induction of a ~50 kDa protein. After an initial drop in expression (72-120 h), the 50 kDa protein was highly expressed during lytic phase (>261 h), concomitant with spikes in caspase specific activity (Fig. 3.3 b). The decrease in 36 kDa protein was concomitant with the increase in 50 kDa protein. This EhMC immuno-hybridization pattern closely resembled that observed for *Ehux* 374 infection with EhV1 (Fig 3.3 a), where both metacaspase-like proteins were expressed initially, followed by a sharp increase in the intensity of the ~50 kDa protein and disappearance of ~36 kDa protein

during the lytic phase. Hence, it is noteworthy that these metacaspases are similarly expressed and regulated by viral infection in two independent sensitive strains (*Ehux374* and *Ehux1516*). This observation further suggests that metacaspases may be responsible for the observed elevated caspase activity in these strains (this study; Bidle et al. 2007).

With the induced caspase activity and metacaspase expression data in this *Ehux1516* and EhV86 host-virus model system, we were poised to employ a genome-enabled, proteomic approach to identify caspase-associated proteins. Our strategy was to take a traditional biochemical purification approach combined with mass spectrometry analysis. Given that both *Ehux1516* and EhV86 have their genomes available, we were able to work back into their respective genomes and identify the genomic signatures. Given that we were initially taking a traditional biochemical approach to isolate caspase-associated proteins, we needed to work out some methodological details. First, proteolysis is a major problem for the purification of proteins, and protease inhibitors could guard against the degradation of target proteins. However, given that caspases are cysteine aspartate specific proteases, we tested whether protease inhibitors could be added to caspase-active lysates and retain activity. This might guard against degradation of our desired proteins with time. A number of protease inhibitors are available that can act on the various proteases, but, it was unknown whether they would inhibit caspases.

We tested the individual effects of EDTA (0.2mM), PMSF (0.2mM), Leupeptin (1 μg/ml) and Aprotinin (5 μg/ml) on caspase specific activity by pre-incubating cell extracts for 5 min prior to the addition of YVAD-AFC. During these short incubations, we observed a general reduction in YVAD-AFC cleavage. PMSF had the highest "retained" activity (90.1%), followed by EDTA (88.6%), Aprotinin (84.4%), and Leupeptin (79.1%). A mixture of PMSF, Leupeptin and Aprotinin, only retained 65.4% activity. Treatment for 24 hours resulted in much reduced caspase activity, with EDTA and PMSF retaining only 47.3% and 16.3% activities, respectively (Fig 3.4). Aprotinin, Leupeptin, and the mixture of P+L+A, actually generated hydrolysis rates higher than an untreated control. Due to the strong caspase inhibition after 24 hr treatment, and the inexplicable increases on the YVAD-AFC hydrolysis, protease inhibitors were not added to cell extracts during purification process. Rather, protein extracts were kept cold (4 °C) wherever possible.

Purification of proteins associated with caspase activity was initiated through sequential ammonium sulfate precipitation up to 90% saturation. After ammonium sulfate precipitation and dialysis, the total cumulative percentage of recovered protein and caspase activity was 52.2% and 86.2%, respectively. The highest caspase specific activity was recovered in the 70% fraction at 11253 RFU mg^{-1} h^{-1}, a 2-fold increase over the original sample extract (Fig 3.5; Fig 3.8). The 70% recovered $AmSO_4$ fraction was subjected to further purification, using ion exchange chromatography in order to differentiate proteins based on surface charge. After binding to the anion exchange column, proteins were eluted with increasing

concentration of NaCl. Approximately 35.8% of the total activity was recovered in the 500mM NaCl fraction during ion exchange chromatography (Fig 3.6), at 62597 RFU mg^{-1} h^{-1}, a ~6 fold increase in specific activity. Other salt elutions contained only 31.2% of the activity seen in 500mM. The 750mM NaCl fraction (18065 RFU mg^{-1} h^{-1}) was also retained for additional analyses. Given that IEC fractions likely contain a mixture of proteins sizes, we then applied size exclusion chromatography (SEC) to further resolve active proteins by size. Two notable peaks in activity were centered around fraction numbers 15 and 19 in 500mM NaCl fractions (Fig 3.7). Note that the 500mM NaCl and 750mM NaCl fractions generally showed the same peaks around fraction 15 (Fig 3.7). Overall, we detected a ~2 fold increase in caspase specific activity after ammonium sulfate precipitation, a ~6 fold increase after ion exchange chromatography, and an overall increase by 12 fold in purification procedures (Fig 3.8).

Given that our $AmSO_4$-, IEC- and SEC- fractions had activity, we first used dot blot analysis as a sensitive and rapid detection of the presence of metacaspase like proteins. Protein detection using the dot blot protocol is similar to western blotting in that both methods test for immuno-reactive proteins with the EhMC antisera. However, dot blot methodology differs from traditional western blot techniques by not separating protein samples using electrophoresis prior to blotting. Sample proteins were directly spotted onto nitrocellulose membranes and hybridized with the EhMC antibody probe. We took two different approaches in our dot blot analysis of $AmSO_4$ precipitation fractions. Both equal amounts of caspase activity (RFU h^{-1}) and equal amounts of protein (0.25μg) were separately spotted onto the

membrane (Fig 3.9 a). If EhMC-like proteins were responsible for caspase activity, then we should see a relatively equal signal among spots loaded with equal caspase activity. At the same time, we should see a spike in immunoreactivity with the highest active fraction when loaded on equal protein basis. For the assay of equal amounts of caspase activity (Fig 3.9 a; right), four of five dots showed more or less the same hybridization intensities. For the assay of equal amounts of protein (Fig 3.9 a; left), the 70% $AmSO_4$ fraction showed the most intense hybridization dot. Likewise, when equal amounts of protein (0.12μg) from IEC fractions were spotted on the nitrocellulose membrane (Fig 3.9 b), the 500mM fraction showed the most intense signal. The 150mM, 250mM, 750mM, and 2M fractions had lower amount of immuno-hybridization, and 1M, 1.5M did not have visible signal. A similar analysis with equal amounts of protein was also performed for SEC fractions but the western blot did not show a signal for SEC caspase active fractions from the 500mM IEC eluates. This is likely due to technical problem with the dot blots procedure or the small volumes of eluates used in this experiment.

In order to identify proteins associated with caspase activity, we subjected purified fractions number 14 in SEC (Fig 3.7; ~1.2 μg with caspase specific activity at 18037 RFU mg^{-1} h^{-1}) to SDS-PAGE and mass spectrometry analysis. Following SDS-PAGE and SilverSNAP staining, we detected 9 distinct bands (Fig 3.10; estimated molecular sizes from 25-120 kDa, designated E3-E12). Using a range of BSA (10-50 ng) as a test case for the sensitivity and detection limit of silver stained gel, we estimated that each band contained ~10-100 ng protein (Fig 3.10). Each band was

excised and submitted to the CABM for mass spectrometry analysis. Using the publically available, *E. huxleyi* 1516 genome database (JGI), several *Ehux1516* proteins were identified based on peptide hits. Interestingly, none of the peptide hits were homologues to metacaspases. A high log(e) value -28.5 identify Band E10 to be *Ehux1516* actin. Other low log (e) (<-3.0) proteins were homologues to kinesin-like protein, phosphoglycerate dehydrogenase, DnaJ, and ceramide synthase among others (Table 3.2). Unfortunately, our low protein amounts and persistent keratin contamination at CABM, limited our resolution and strength of protein hits.

As an alternative, we contacted colleagues at MUSC who had previous success with proteomics of the diatom *Fragilariopsis cylindrus* (M. Janech, personal communication). Four samples were submitted to MUSC for proteomics analysis using 2D GE and MALDI-TOF-TOF. These fractions included (1) a pooled subset of caspase active fractions from SEC 500mM (Fig 3.7; Fraction numbers 13-22), (2) a pooled subset of caspase active fractions from SEC 750mM (Fig 3.7; Fraction numbers 12-18), (3) a pooled subset of non-active fraction (Fig 3.7; SEC 500mM fraction number 29; 'negative control'), and (4) a 6x His-tagged purified recombinant *E. huxleyi* metacaspase (EhMC; Protein ID 440238; 'positive control'). SYPRO-Ruby staining of 2D gels generated clear resolution of 10-17 spots in caspase-active fractions; notably, caspase-active fractions yielded the same spot pattern (Fig 3.11; A, B ; Fig 3.12; A, B). In contrast, only one spot was observed in caspase-negative fractions (Fig 3.11 C; Fig 3.13 A). The EhMC recombinant protein yielded a spot with the expected IP of 5.2 and molecular weight of ~41 kDa (Fig 3.11 D; Fig 3.13 B). In all, thirty-one spots exceed a

user defined intensity threshold for successful identification and were picked for mass spectrometry analysis using MASCOT. Peptides were searched against the publically available, web-based sequence databases from the *E. huxleyi CCMP1516* and *E. huxleyi* virus 86 genome projects (http://www.ncbi.nlm.nih.gov/sites/entrez?Db=genome&Cmd=Retrieve&dopt=Protein+Table&list_uids=18666).

Mass spectrometry analysis returned peptide hits to hundreds of putative *Ehux1516* proteins. Notably, none of the peptide hits corresponded to annotated EhMCs. Nonetheless, seventeen proteins hits, including four from the EhV86 proteome, were homologues to proteases or death related proteins (Table 3.3). For example, peptide fragments for spot# 5201 (Fig 3.12 B) had a blast score of 34.3 to a marine actinobacterium serine protease (Table 3.3). In addition, peptide fragments for spot# 5502 (Fig 3.12 B) yielded a blast score of 38.5 to an *Aspergillus fumigatus* OTU-like cysteine protease (Table 3.3). It is possible that these proteins confer caspase activity, especially the latter example since it is a closely related cysteine protease. Interestingly, none of the peptide hits from the purified recombinant *E. huxleyi* metacaspase (Fig 3.13 B) were homologues to protein ID 440238, which suggests the possibility that proteins were dramatically modified (i.e., glycosylation /phosphated /prenylated /acetylated /ubiquitinated) or that errors exist in the JGI database, thereby making identification difficult, Such errors could possible explain the poor resolution of our 1D SDS-PAGE analysis.

Clearly, future work on these promising protein targets needs to be performed in order to confirm activity and elucidate their putative function. The development of a transformation system for *E. huxleyi* would greatly aid in this endeavor. For example, transformation (via biolistic delivery) and overexpression of these proteins (Table 3.3) in *E. huxleyi* and subsequent measurements of caspase specific activity would directly test our hypothesis. Additionally, physiological and biochemical characterizations of gene knockouts would definitively elucidate the activity and function of these gene products.

Table 3.1 Host range of the *Emiliania huxleyi* virus (EhV) isolates to *E. huxleyi* host strains from the CCMP culture collection (http://ccmp.bigelow.org/) (Table adapted from Schroeder et al. 2002) and comparison of *E. huxleyi* location of isolation.

Virus isolate	*E. huxleyi* host[1]					
	CCMP 370	CCMP 373	CCMP 374	CCMP 379	CCMP 1516	L
*Eh*V84	□	□	+	□	+	+[2]
*Eh*V86	□	□	+	□	+	+[2]
*Eh*V88	□	□	+	□	+	+[2]
*Eh*V163	□	□	+	□	+	+
*Eh*V201	□	□	+	□	+	+
*Eh*V202	□	□	+	□	+	+
*Eh*V203	□	□	+	□	□	+
*Eh*V205	□	□	+	□	+	□
*Eh*V207	□	□	+	□	+	+[2]
*Eh*V208	□	□	+	□	+	+

[1]Culture lysis (+); No evidence of culture lysis (□);
[2]Culture lysis very slow when compared to the other lysed cultures

E. huxleyi strain ID	Location of isolation
CCMP370	North Atlantic, Fjord, Norway
CCMP373	North Atlantic, Sargasso Sea
CCMP374	North Atlantic, Gulf of Maine
CCMP379	North Atlantic, Eddystone, English Channel
CCMP1516	South Pacific

based on information from the Provasoli-Guillard National Center for Culture of Marine Phytoplankton (CCMP); https://ccmp.bigelow.org/

Table 3.2: Top protein hits from 1D SDS-PAGE and mass spectrometry analysis of caspase-active fractions

Band #	Protein ID[a]	log (e)	Putative function[b]
E3	209453|gm1.3900179	-1.1	hypothetical protein/unnamed protein product
E5	217953|gm1.7600086	-2	D-3-phosphoglycerate dehydrogenase
	412392|estExt_fgenesh_newKGs_kg.C_4020006	-1.4	hypothetical protein
	199077|gm1.900269	-1.2	hypothetical protein/Cytochrome c5
	97394|fgeneshEH_pg.10__18	-1.1	hypothetical protein
	269074|estExt_fgeneshEH_pg.C_430051	-1.1	pseudouridylate synthase
E6	105570|fgeneshEH_pg.69__94	-1.2	predicted protein [Thalassiosira pseudonana]
E7	214133|gm1.6000071	-1.4	unknown
	220149|gm1.8900174	-1.2	hypothetical protein
E8	269589|estExt_fgeneshEH_pg.C_580072	-1.5	No significant similarity found
	199074|gm1.900266	-1.6	No significant similarity found
	125341|fgeneshEH_pg.9231__1	-1.5	hypothetical protein
	202422|gm1.1600238	-1.2	pyruvate dehydrogenase/dihydrolipoamide S-acetyltransferase
	208971|gm1.3700023	-1.2	serine/threonine protein kinase
	231068|gm1.16900054	-1.2	putative protein kinase
	357644|fgenesh_newKGs_kg.60__103 __EST_ALL.fasta.Contig9117	-1.1	calmodulin
	276494|estExt_Genemark1.C_120341	-1.1	PfkB domain protein/ribokinase-like domain-containing protein
E10	196492|gm1.400614	-28.5	type 1 actin [Emiliania huxleyi]
	123872|fgeneshEH_pg.3391__1	-3.4	predicted protein/Scaper protein
	217107|gm1.7200120	-2.2	predicted protein/kinesin-like protein
	221829|gm1.9900038	-2.1	hypothetical protein/fungal specific transcription factor
	282962|estExt_Genemark1.C_1880006	-1.5	Phox/Bemp1 (PB1) domain-containing protein
	218491|gm1.7900153	-1.3	unnamed protein product
	214609|gm1.6200048	-1.2	short chain dehydrogenase/putative glycosyltransferase
	278091|estExt_Genemark1.C_340041	-1.1	No significant similarity found
E11	410043|estExt_fgenesh_newKGs_kg.C_1720001	-2.2	No significant similarity found
	123588|fgeneshEH_pg.2634__1	-2.1	kinetoplast-associated protein-like protein
	209370|gm1.3900096	-1.1	No significant similarity found
	269560|estExt_fgeneshEH_pg.C_570056	-1.1	No significant similarity found
E12	230109|gm1.16100037	-1.9	DnaJ (Hsp40) homolog, subfamily B
	214144|gm1.6000082	-1.4	ceramide synthase

[a] http://genome.jgi-psf.org/Emihu1/Emihu1.home.html

[b] Based on the best pBLAST hits (http://blast.ncbi.nlm.nih.gov/Blast.cgi)

Table 3.3: Putative protease and PCD-like proteins from 2D GE and mass spectrometry analysis of caspase-active fractions

Spot #	Gel #	Protein ID[a]	Protein score	Blast score[b]	Putative function[b]
3303	1	249208|gm1.75200003 RANDOM	34	36.6	zinc-binding carboxypeptidase [*Streptomyces viridochromogenes* DSM 40736]
5604	1	229266|gm1.15400062 RANDOM	28	84.7	Peptidase S53 propeptide [*Chthoniobacter flavus* Ellin428]
6401	1	EhV154 hypothetical protein 142093:142836 forward	14	43.1	putative peptidoglycan peptidase [*Flavobacterium johnsoniae* UW101] [*Pelobacter propionicus* D
7201	1	EhV018 putative endonuclease 12303:13379 reverse	14	320.0	Cell-death-Related Nuclease family member (crn-1) [*Caenorhabditis elegans*]
7401	1	439410|estExtDG_fgenesh_newKGs_kg.C_990066 RANDOM	23	37.0	similar to ubiquitin specific protease 42 [*Taeniopygia guttata*]
		EhV037 putative membrane protein 35982:36506 reverse	14	35.0	Peptidase, family M23/M37 [Bacillus pseudomycoides DSM 12442] [*Clostridium cellulovorans* 74
2703	2	437422|estExtDG_fgenesh_newKGs_kg.C_590027 RANDOM	30	36.2	X-Pro dipeptidyl-peptidase domain-containing protein [*Salinispora arenicola* CNS-205]
3302	2	234709|gm1.20700055	42	35.4	peptidase U32 [*Dickeya dadantii* Ech586/703]
3701	2	207840|gm1.3200290	30	35.0	serine protease, subtilase family protein [*marine actinobacterium* PHSC20C1]
		218945|gm1.8100175 RANDOM	25	36.6	UfSP2 peptidase (C78 family) [*Schistosoma mansoni*]
5201	2	458815|estExtDG_Genemark1.C_3830028 RANDOM	25	34.3	similar to Adipocyte-derived leucine aminopeptidase precursor (A-LAP) (ARTS-1) [*Gallus gallus*]
5502	2	98149|fgeneshEH_pg.13__32	27	47.4	UBP19 (UBIQUITIN-SPECIFIC PROTEASE 19); cysteine-type endopeptidase[*Arabidopsis thalia*
		314539|fgenesh_newKGs_pm.184__16	25	67.0	death associated protein kinase [Equus caballus] [Rattus norvegicus][*Mus musculus*]
		460476|estExtDG_Genemark1.C_12030002 RANDOM	26	38.5	OTU-like cysteine protease [*Aspergillus fumigatus* Af293]
		232231|gm1.17900085 RANDOM	24	36.2	putative metalloendopeptidase (ISS) [*Ostreococcus tauri*]
		EhV461 putative membrane protein 401427:402338 forward	13	36.2	peptidase U35 phage prohead HK97 [*Natrialba magadii* ATCC 43099]
5503	2	455217|estExtDG_Genemark1.C_1360067 RANDOM	33	40.8	O-sialoglycoprotein endopeptidase [*Bacillus pseudomycoides* DSM 12442]

[a] http://genome.jgi-psf.org/Emihu1/Emihu1.home.html
http://www.ncbi.nlm.nih.gov/sites/entrez?Db=genome&Cmd=Retrieve&dopt=Protein+Table&list_uids=18666

[b] Based on the best pBLAST hits (http://blast.ncbi.nlm.nih.gov/Blast.cgi)

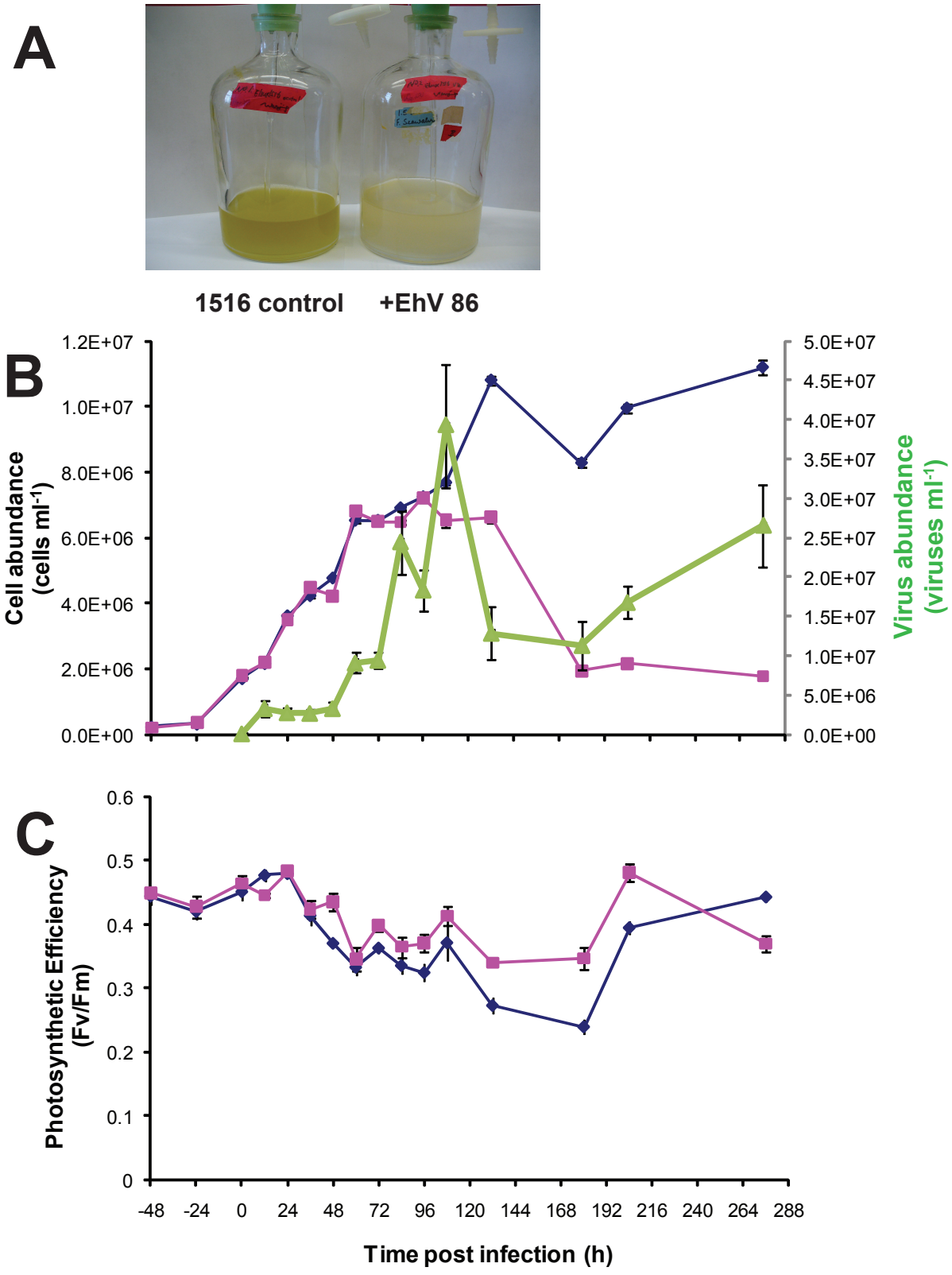

Figure 3.1: Dynamics of EhV86 infection of *Ehux1516*. (A) Visual comparison of control (left) and infected cultures (right) 276 h post infection. (B and C) Time course of growth (B) and photosynthetic efficiency (C) for uninfected control (blue lines) and EhV86 infected cultures (purple lines). Green lines represent virus abundance. Error bars represent standard deviation from triplicate measurements.

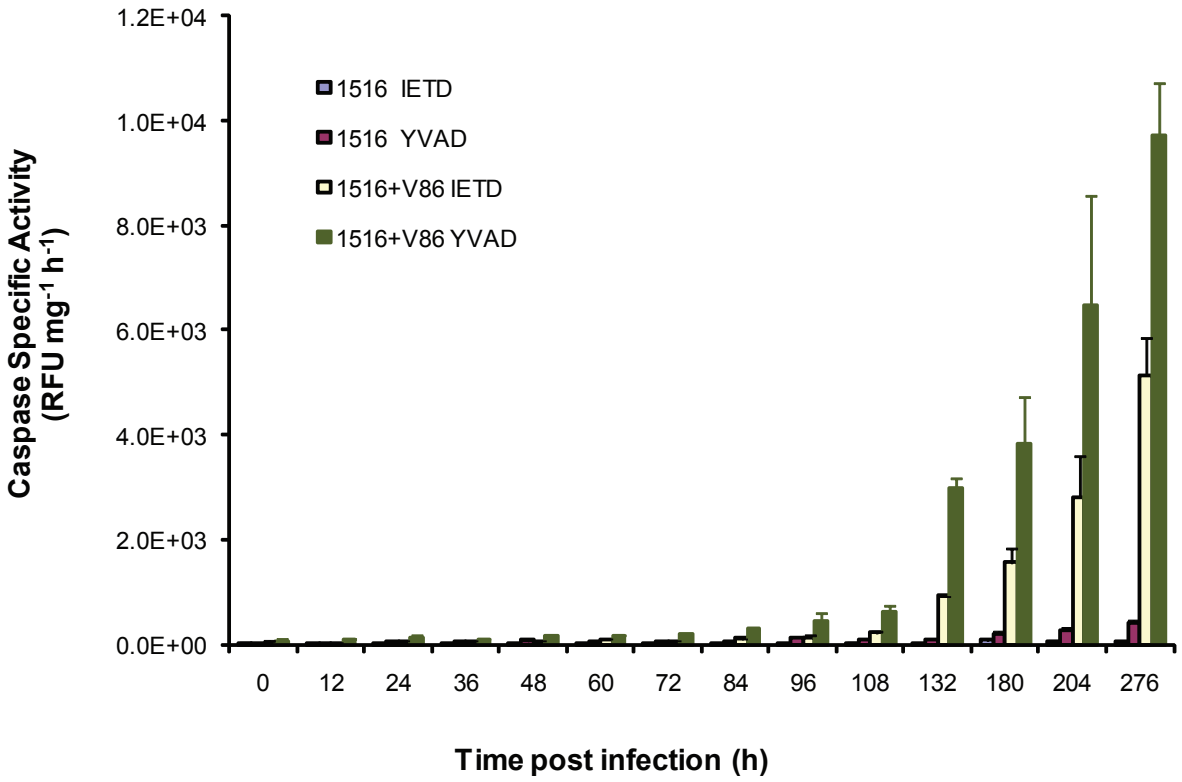

Figure 3.2: Caspase activation in *Ehux1516* by EhV86 infection. Green and yellow bars represent caspase-specific activity in infected cell extracts as measured by the cleavage of YVAD-AFC and IETD-AFC, respectively. Red and blue bars represent caspase specific activity in control cell extracts with the same respective fluorogenic substrates. Note that YVAD-AFC yielded twice the level of caspase activity than IETD-AFC. Error bars represent standard deviations among triplicate measurements.

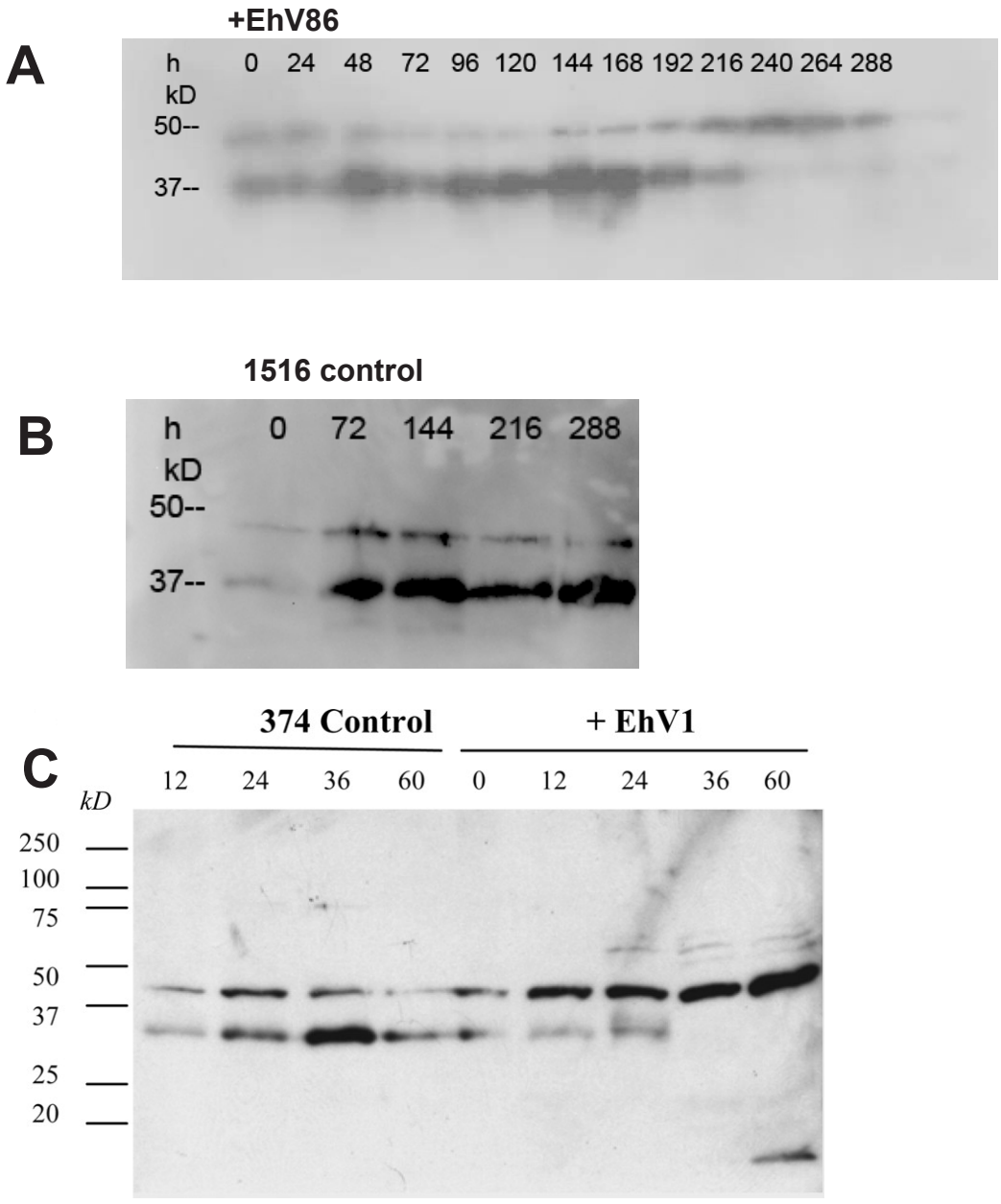

Figure 3.3: Detection of metacaspase expression in sensitive *E. huxleyi* strains during viral infection. (A) and (B) Western blot analysis of *Ehux1516* cell extracts collected during a time course of EhV86 viral infection and uninfected control cell extracts, showing immunohybridization to polyclonal antisera generated against a purified, recombinant *E. huxleyi* metacaspase protein (EhMC). (C) Western blot analysis of *Ehux374* infected with EhV1 (as adapted from Bidle et al. 2007). Lane numbers represent collection time (hours post infection). Note similar dynamic expression patterns of both ~50 kD and ~36 kD metacaspase-like proteins, with elevated expression of ~50 kD protein during late phase infection.

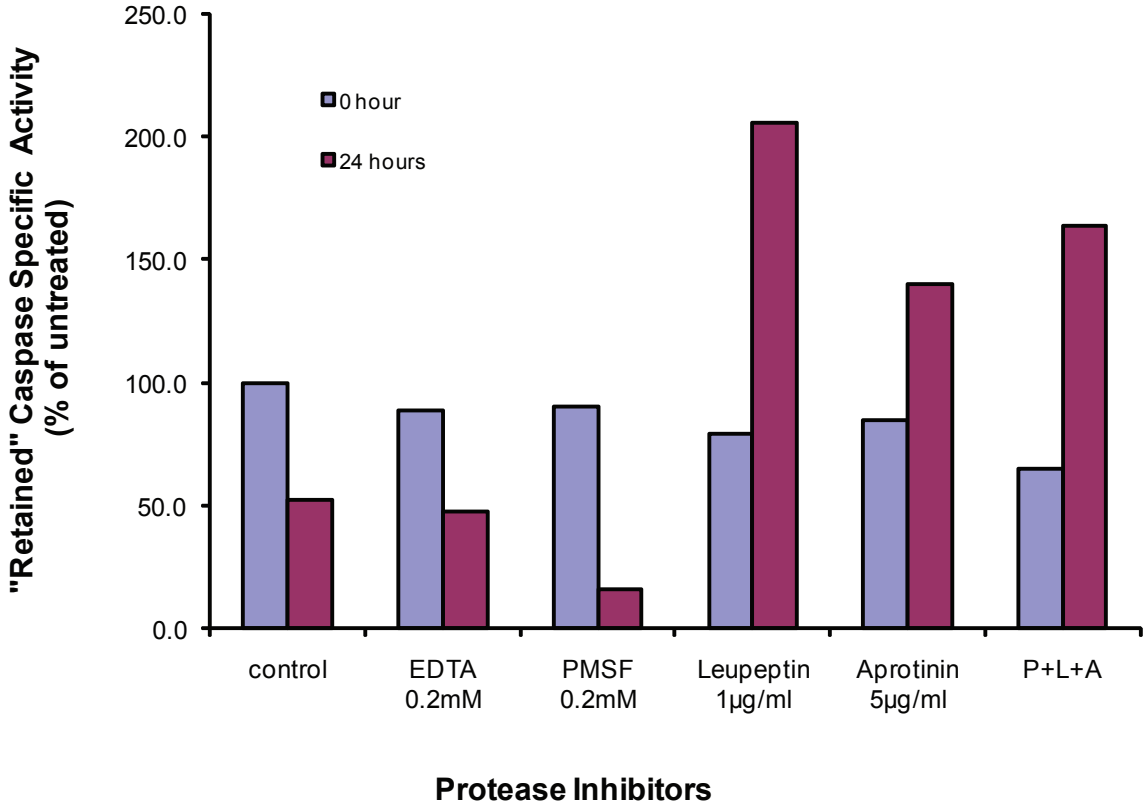

Figure 3.4: The effect of protease inhibitors on caspase specific activity. After protease inhibitors were added to cell extract and incubated for the specified time period (see legend), caspase specific activities were measured via hydrolysis of the fluorogenic substrate, YVAD-AFC, and normalized to untreated controls (%).

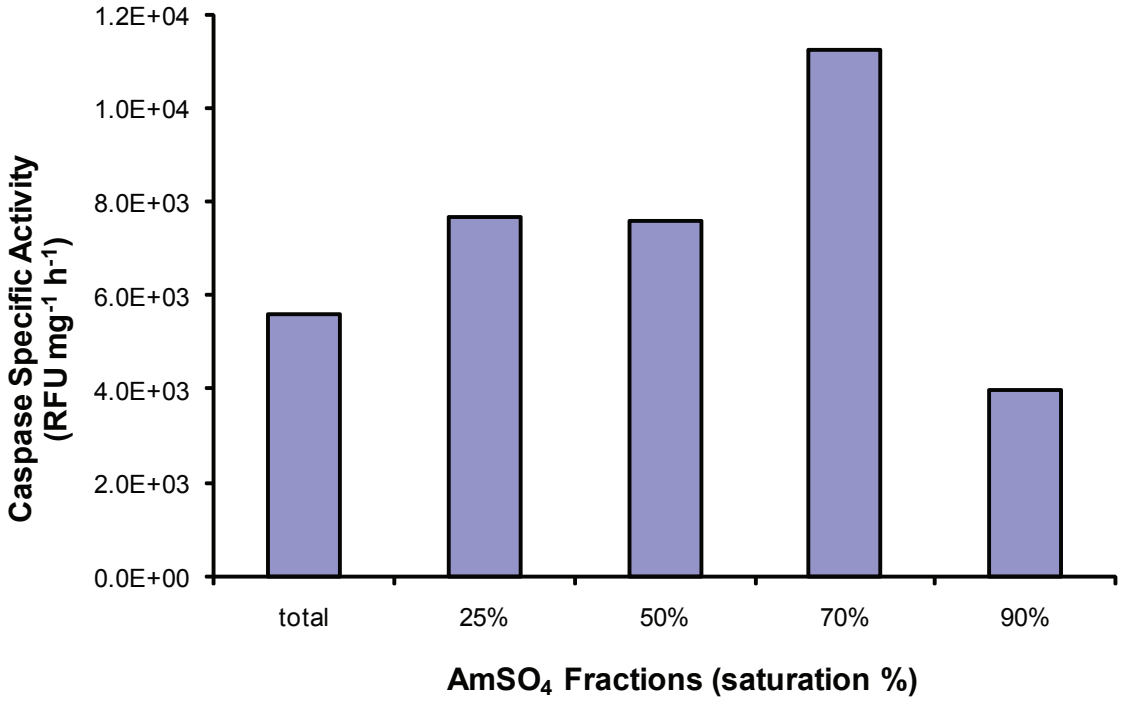

Figure 3.5: Caspase specific activity in fractions after ammonium sulfate precipitation. Ammonium sulfate precipitates were resuspended in PBS buffer and assayed for activity via YVAD-AFC hydrolysis. Fractions above 50% were dialyzed prior to activity assays to remove excess salt. All fractions were normalized to toal protein via BCA protein assay (see methods).

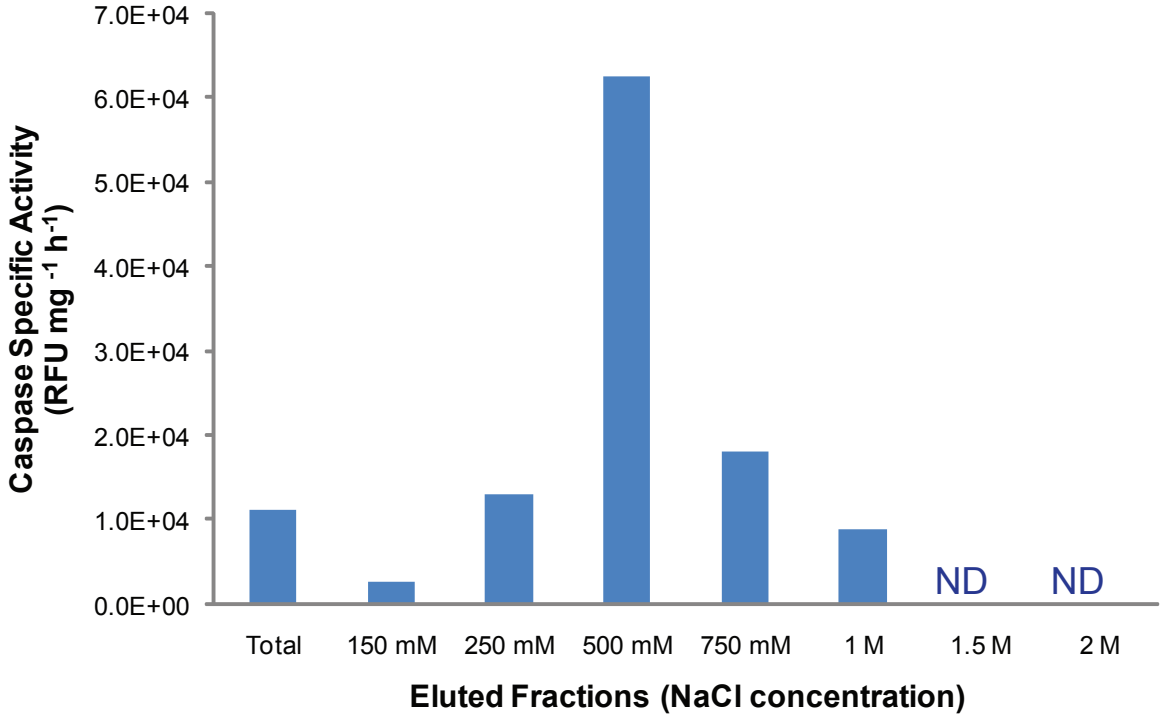

Figure 3.6: Caspase specific activity in eluted fractions after high Q anion exchange chromatography. The 70% $AmSO_4$ fraction was loaded on the IEC column and eluted in a step-gradient of NaCl concentration. All IEC fractions were assayed for activity via YVAD-AFC hydrolysis, and normalized to total protein via BCA protein assay (see methods). "ND" represents none-detected. "Total" represents the $AmSO_4$ fraction loaded on the IEC column.

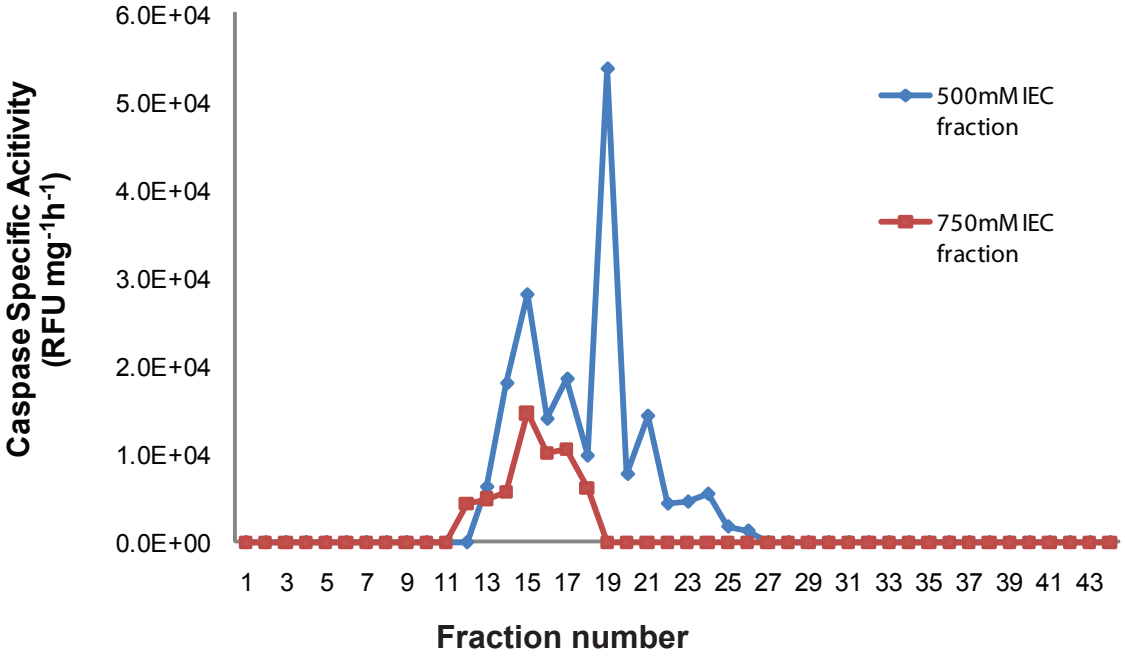

Figure 3.7: Caspase specific activity profile of eluted fractions after P-100 gel filtration chromatography. The 500mM and 750mM fractions from IEC were loaded as starting material and separately subjected to SEC. The elution volume was ~90µl per fraction. All SEC fractions were assayed for activity via YVAD-AFC hydrolysis, and normalized to total protein via UV absorption at 280nnm (A280 assay) (see methods).

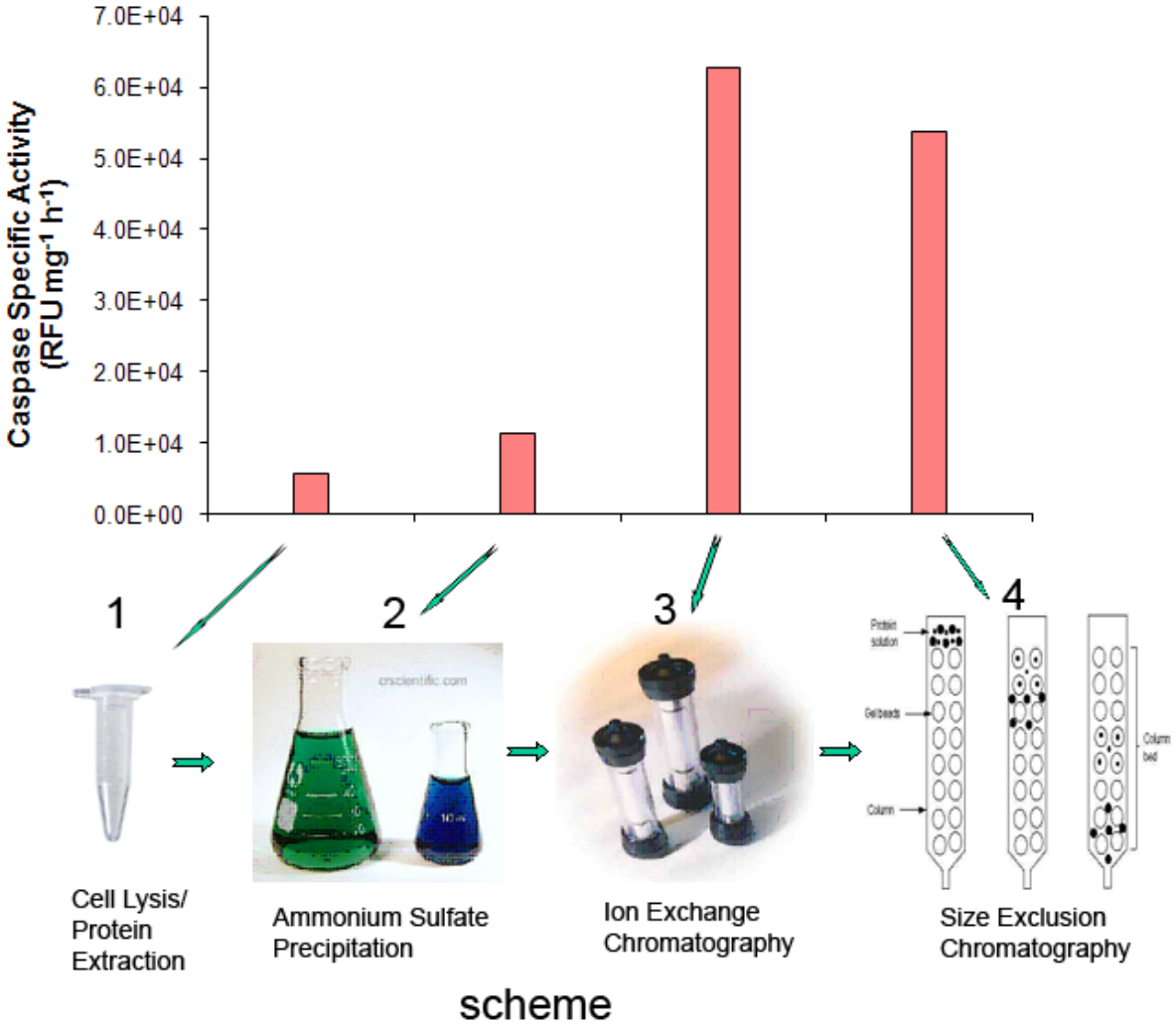

Figure 3.8: Enrichment of caspase specific activity associated with the purification scheme. We observed a general enrichment in caspase specific activity with successive steps of purification. We detected a ~12 fold increase in caspase specific activity after combined ammonium sulfate precipitation, ion exchange chromatography and size exclusion chromatography.

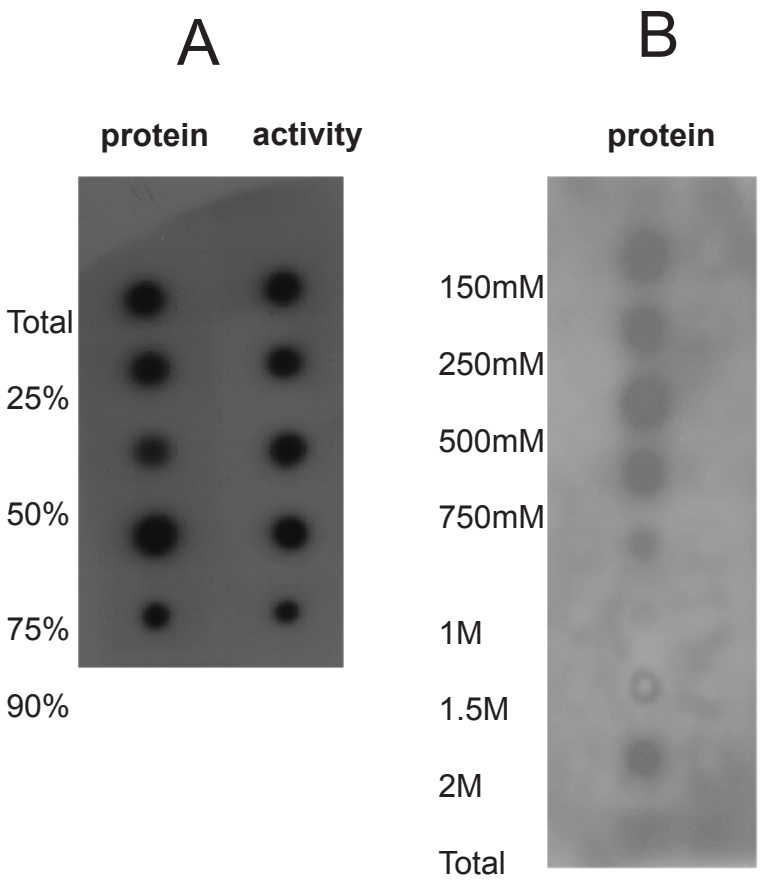

Figure 3.9 Immunohybridization of purification fractions to EhMC antibody. Dot blot analysis of (A) $AmSO_4$ precipitation and (B) IEC purified fractions. For (A), equal protein and equal caspase specific activity were spotted onto the membrane. For (B), equal protein was loaded. In each case, membranes were probed with EhMC antibody.

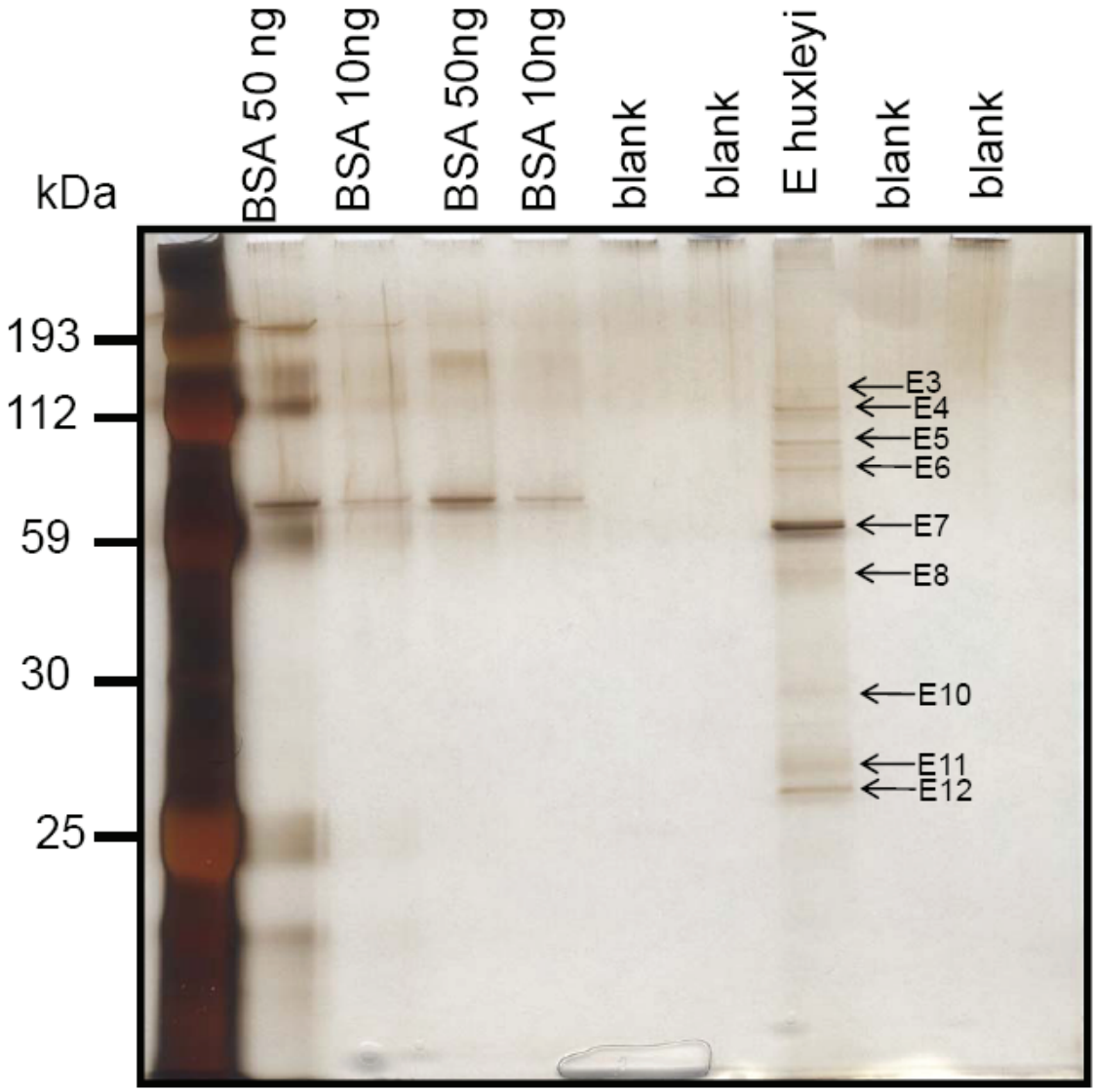

Figure 3.10: Silver SNAP-stained SDS-PAGE of an active SEC fraction showing bands excised for proteomics analysis. Lanes 1 (from left to right) was molecular weight marker. Different concentrations of BSA (10-50ng) were served as controls for sensitivity and detection limit. *E. huxleyi* sample represents fraction No.14 from Fig 3.7 with high caspase specific activity. Visible bands were excised for tryptic-digestion and mass spectrometry analysis (E3-E12).

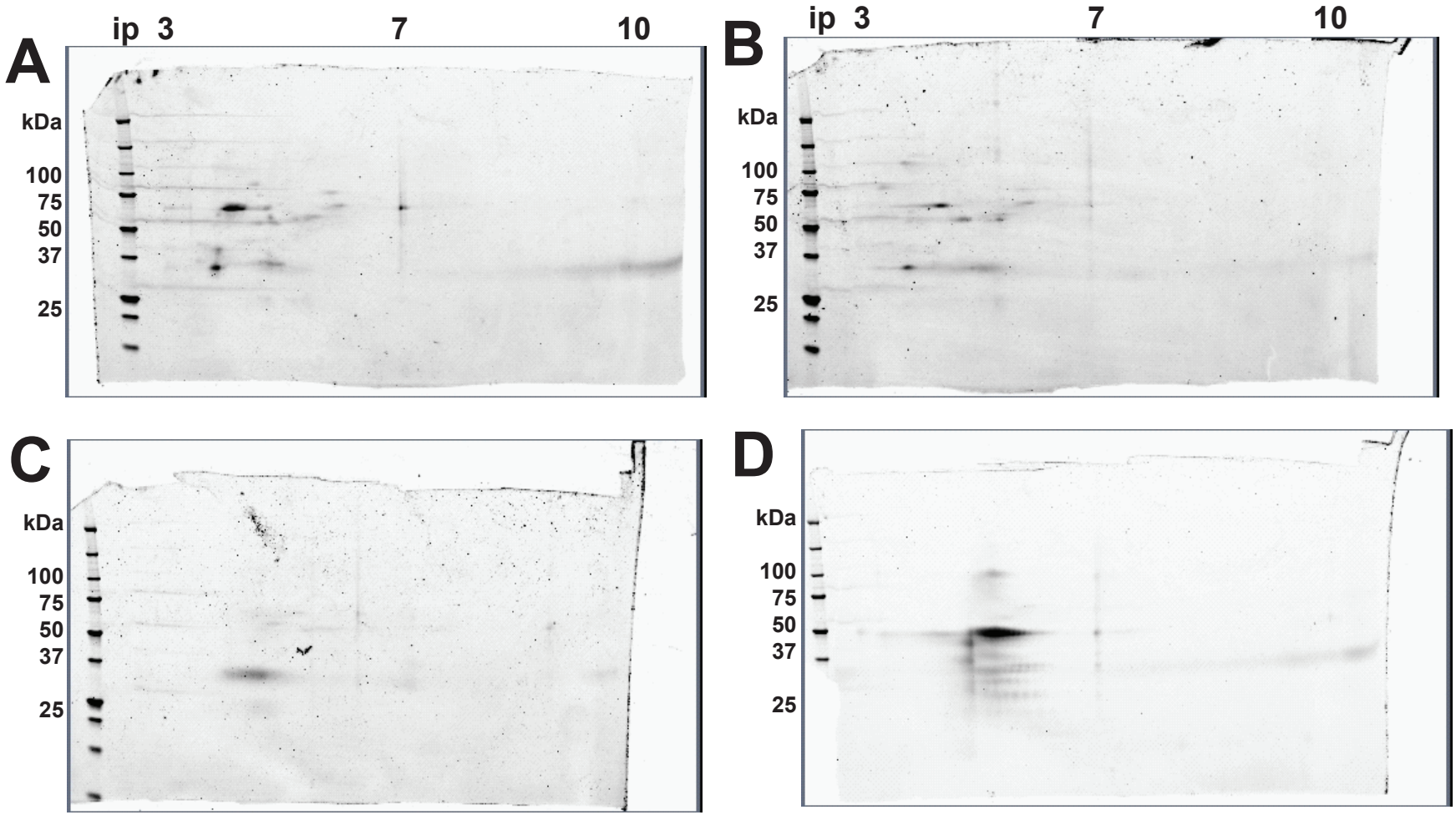

Figure 3.11 Sypro Ruby stained 2D gels of *E.huxleyi* proteins. (A) and (B) represent pooled subsets of post-SEC caspase active fractions from 500mM and 750mM NaCl IEC eluates, respectively. (C) represents a pooled subset of non-active fraction from the 500mM NaCl IEC eluates and serves as a negative control. (D) represents a 6x His-tagged, purified recombinant *E. huxleyi* metacaspase (EhMC; Protein ID 440238) and serves as a positive control for database searches, as well as control for IP and molecular weight in 2D gel. 31 distinct spots above a critical intensity threshold were excised for mass spectrometry analysis. Molecular weight markers and pI are indicated.

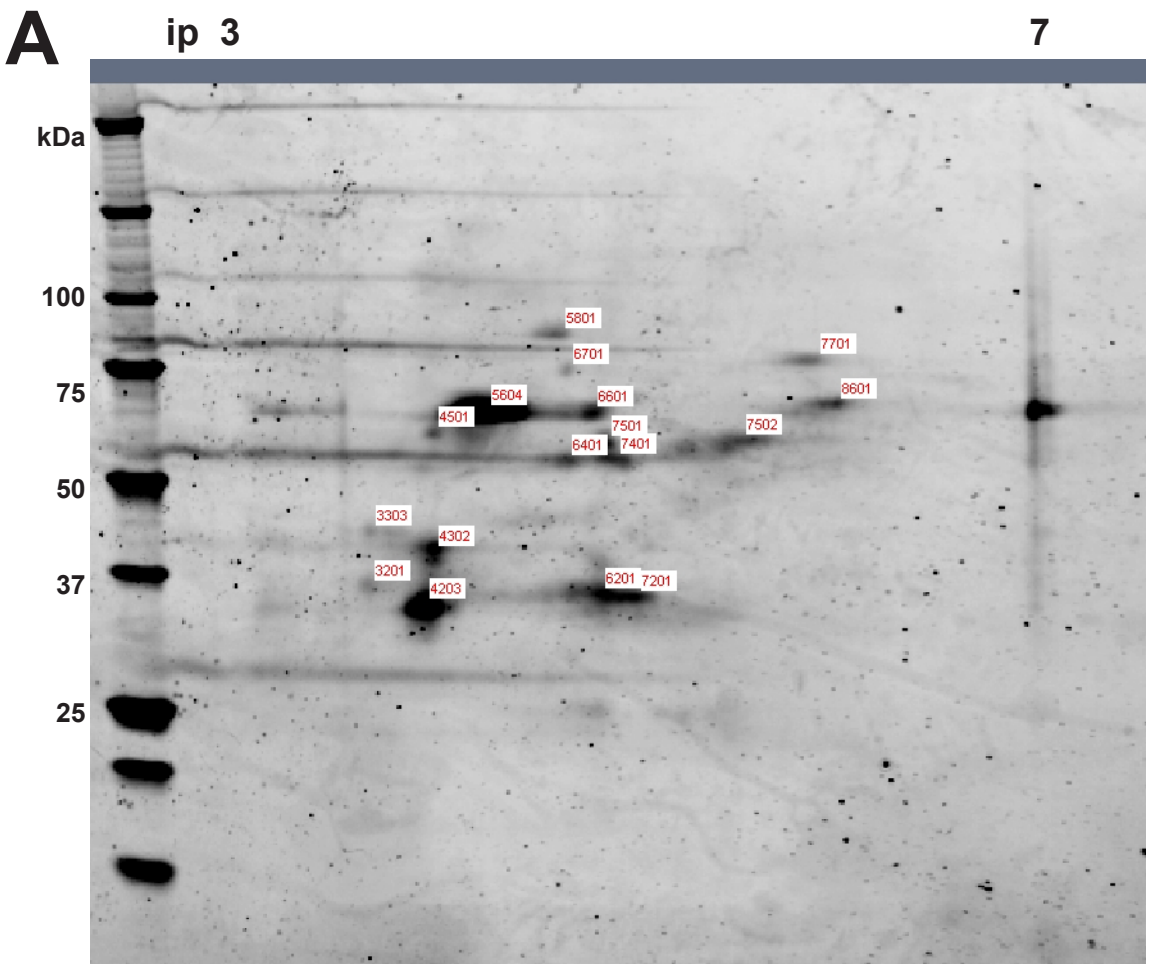
A
ip 3
7
kDa
100
75
50
37
25
5801
6701
5604
6601
4501
7501
6401
7401
7701
8601
7502
3303
4302
3201
4203
6201
7201

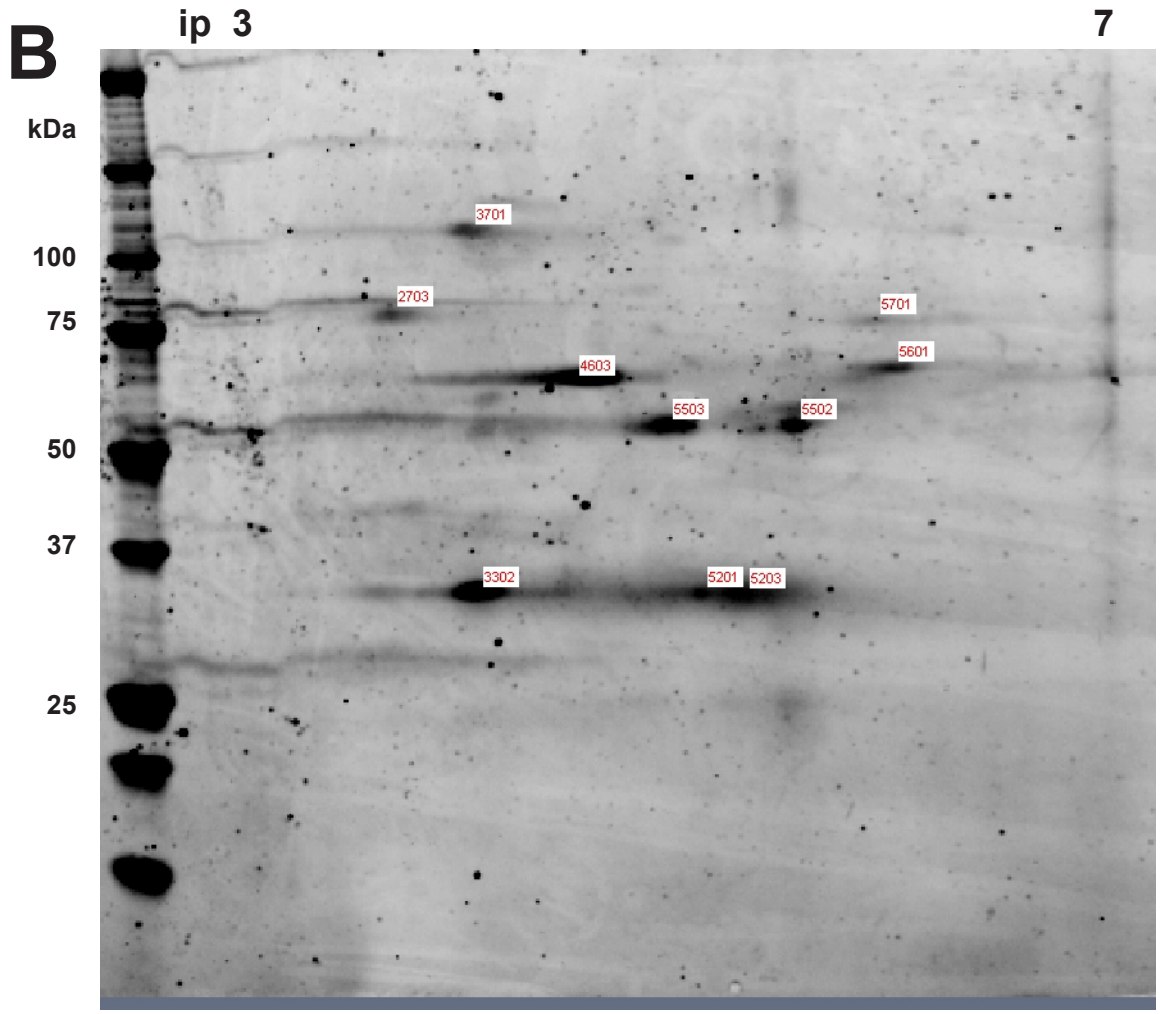

Figure 3.12 Sypro Ruby stained 2D gel of *E.huxleyi* proteins associated with caspase activity. A subset of pooled post-SEC caspase active fractions from 500mM (A) and 750mM (B) NaCl IEC eluates. Seventeen and ten distinct spots, respectively (indicated by spot numbers), were above a critical intensity threshold and were excised for mass spectrometry analysis. Molecular weight markers and pI are indicated.

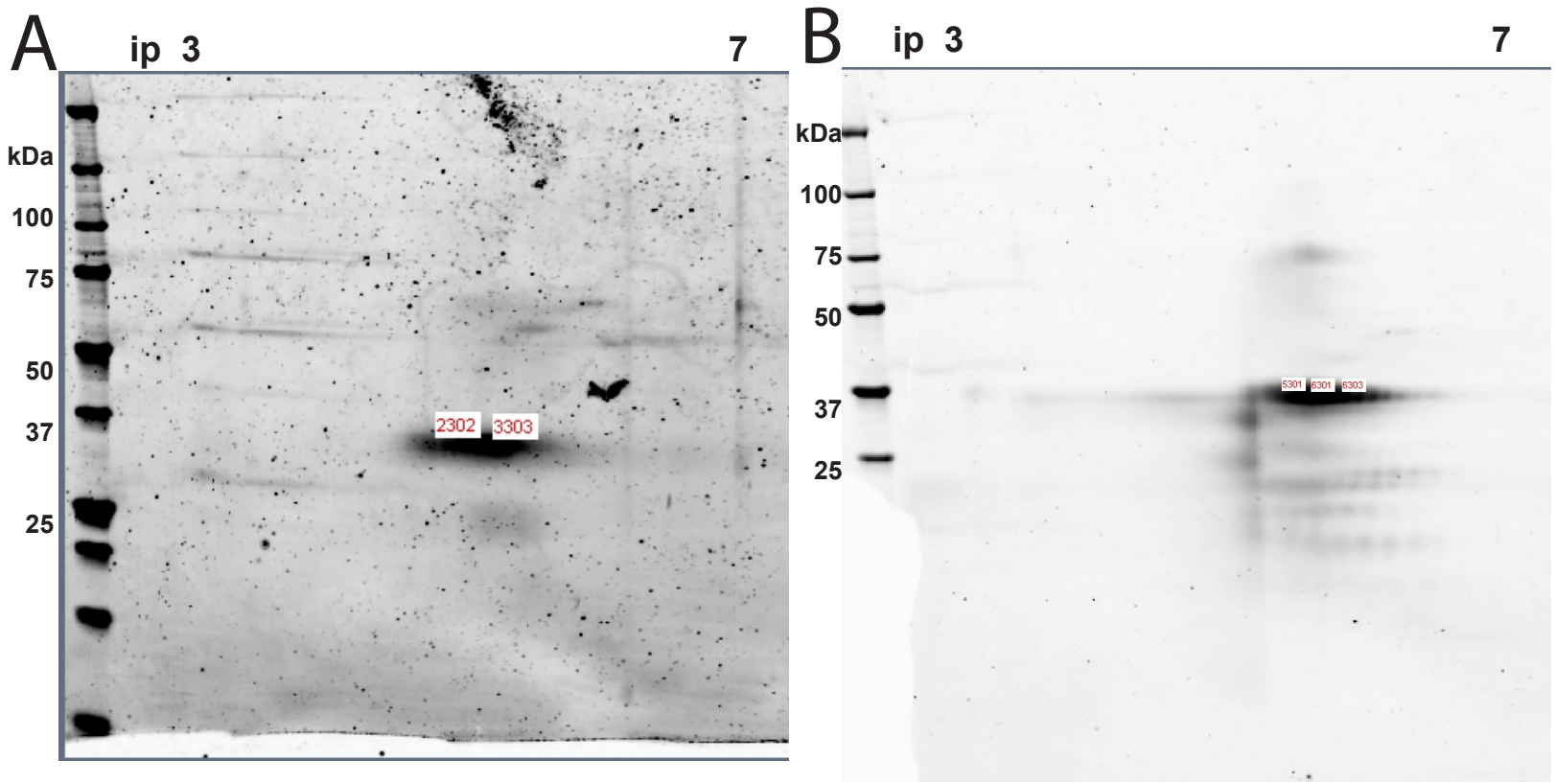

Figure 3.13 Sypro Ruby stained 2D gel of *E.huxleyi* control proteins. (A) A subset of pooled non-active fractions from the 500mM NaCl IEC eluates (negative control). (B) A 6x His-tagged, purified recombinant *E. huxleyi* metacaspase (EhMC; Protein ID 440238), served as a positive control for database searches, and for IP and molecular weight during the 2D gel electrophoresis procedure. Five distinct spots (indicated by spot numbers) were above a critical intensity threshold and were excised for mass spectrometry analysis. Molecular weight markers and pI are indicated.

References:

Allen M.J. D. C. Schroeder, M. T. G. Holden, & W. H. Wilson. (2006). Evolutionary History of the *Coccolithoviridae*. *MOLECULAR BIOLOGY AND EVOLUTION.* **23** (1)**:** 86-92.

Bidle K. D. L. Haramaty, J. B. e Ramos, & P. G. Falkowski. (2007). Viral Activation and Recruitment of Metacaspases in the Unicellular Coccolithophore, *Emiliania Huxleyi*. *Proc. Natl. Acad. Sci.* **104** (14)**:** 6049-6054.

Bidle K. D. & P. G. Falkowski. (2004). Cell Death in Planktonic Photosynthetic Microorganisms. *NATURE REVIEWS: MICROBIOLOGY.* **2:** 643-655.

Englard S. & S. Seifter. (1990). Precipitation Techniques, Guide to Protein Purification, Methods in Enzymology. **182:** 291.

Madeo F. E. Herker, *et al*. (2002). A Caspase-Related Protease Regulates Apoptosis in Yeast. *MOLECULAR CELL.* **9:** 911-917.

Schroeder D. C. J. Oke, G. Malin, & W. H.Wilson. (2002). Coccolithovirus (*Phycodnaviridae*): Characterisation of a New Large Dsdna Algal Virus That Infects *Emiliania Huxleyi*. *ARCHIVES OF VIROLOGY.* **147:** 1685-1698.

Szalliesa A. B. K. Kubatac, & M. Duszenkoa. (2002). A Metacaspase of *Trypanosoma Brucei* Causes Loss of Respiration Competence and Clonal Death in the Yeast *Saccharomyces Cerevisiae*. *FEBS LETTERS.* **517:** 144-150.

Teodoro J. G. & P.E. Branton. (1997). Regulation of Apoptosis by Viral Gene Products. *JOURNAL OF VIROLOGY.* **71** (3)**:** 1739-1746.

Vardi A., B. A. S. Van Mooy, et al. (2009). Viral Glycosphingolipids Induce Lytic Infection and Cell Death in Marine Phytoplankton. *SCIENCE.* **326:** 861 - 865.

Vercammen D. vdB. Cotte, et al. (2004). Type Ii Metacaspases Atmc4 and Atmc9 of *Arabidopsis Thaliana* Cleave Substrates after Arginine and Lysine.

JOURNAL OF BIOLOGICAL CHEMISTRY. **279** (44)**:** 45329-45336.

Wilson W. H. D. C. Schroeder, *et al*. (2005). Complete Genome Sequence and Lytic Phase Transcription Profile of a *Coccolithovirus*. *SCIENCE.* **309:** 1090-1092.

4.0 Summary

In this thesis, physiological and biochemical approaches combined with proteomics and mass spectrometry were applied to *Emiliania huxleyi* and four other phytoplankton species in an effort to understand how metacaspases are expressed in diverse phytoplankton species and to link observed caspase specific activities in *E. huxleyi* with genetic signatures.

We observed typical batch culture growth dynamics in four phytoplankton species, including a chlorophyte (*Dunaliella tertiolecta*), a haptophyte (*Isochrysis galbana),* a diatom (*Thalassiosira weissflogii*), and a dinoflagellate (*Amphidinium carterae*). Specific growth rates generally correlated with caspase specific (IETD-AFC hydrolysis) activity, and caspase activity generally increased 3-12 fold with stationary and death phase in all species. An *E. huxleyi* metacaspase (EhMC) antibody, the first polyclonal antibody generated specifically against phytoplankton metacaspases, was used to investigate metacaspase expression in these four different ecologically and evolutionarily diverse eukaryotic phytoplankton species (primary, secondary and tertiary endosymbionts), none of which has whole genome information presently available. Western blot analysis detected distinct bands for all species tested, indicating metacaspase-like proteins are expressed in diverse phytoplankton, and affirming the widespread presence of metacaspases in unicellular phytoplankton. These metacaspases responded under different physiological environmental stresses. *D. tertiolecta* revealed expression of one EhMC-like protein, resembling *D. tertiolecta* extracts probed with

human caspase 8 antibody (Segovia 2003). *I. galbana*, showed the most pronounced death and possessed protein expression which strongly correlated with elevated caspase activity. The diatom, *T. weissflogii*, showed the highest range of caspase specific activity and had multiple distinct bands, some of which are similar to the pattern of *T. pseudonana* (Bidle & Bender 2008). The dinoflagellate, *A. carterae*, showed the most expressed bands (total bands >7). Some protein was constitutively expressed in all phases, and at least 3 proteins were downregulated at the beginning of death phase. A general accumulation in the diversity of metacaspase expression was found in samples ranging from a primary (*D. tertiolecta*), and secondary (*I. galbana* and *T. weissflogii*) to the most derived tertiary (*A. carterae*) endosymbiotic phytoplankton lineages. Metacaspase-like protein expression did not always correlate with elevated caspase activities, which suggests some of these EhMC antibody hybridized proteins are associated with caspase-like activity and executing death, others may not. It also indicates that metacaspases may have different physiological roles.

Even though the presence and expression of metacaspases, as well as the induction of caspase activity, are widespread in diverse phytoplankton, to date, there has been no direct link with metacaspases genes. Therefore, we took advantage of recent observations on the co-evolution of *Ehux*1516 and EhV86 virus-host interactions in the activation of PCD. We observed dramatically decreased cell abundance and Fv/Fm 120 hrs post infection and a dynamic affect on the expression of two EhMC-homologue proteins. EhV86 infection specifically triggered a sharp increase in the intensity of a 50 kDa protein, correlating with caspase specific activity, and a

concomitant decrease in a 36 kDa protein. The pattern paralleled that seen in EhV1 infected *E.huxleyi* 374.

Using a genome enabled approach, we linked caspase activities to genomic signatures. Cell extracts collected during late lytic phase of viral infection showed enrichment in caspase activity with successive steps of biochemical purification. Overall, we detected a ~12 fold increase in caspase specific activity after ammonium sulfate precipitation, ion exchange chromatography and size exclusion chromatography. SEC purified fractions that possessed caspase specific activities as high as 5×10^5 RFU mg^{-1} h^{-1} were subjected to both denaturing SDS-PAGE and 2D GE followed by mass spectrometry analysis. Protein IDs from 1D SDS-PAGE showed hits to a variety of diverse proteins, including actin, kinesin-like protein, and ceramide synthase. We did not have peptide hits to any metacaspase. The poor resolution was likely due to low protein amounts and persistent keratin contamination. On the other hand, 2D GE yielded multiple spots in caspase-active fractions. Based on this analysis, 2D GE showed many more hits to diverse *E.huxleyi* and EhV86 proteins, including seventeen proteins hits, which were homologues to proteases or death related proteins. It suggests these protease-like proteins may be associated with caspase activity and execute PCD. It also suggests that proteins with caspase-like activity may be virally derived.

In summary, this study demonstrated the importance of metacaspases in diverse lineages of marine phytoplankton and examined the proteins associated with

caspase activity. It also touched on the origin and nature of PCD genes in unicellular photoautotrophs. Given their evolutionary history, biochemical complexity, and largely unknown physiological roles, I am sure people who are interested in phytoplankton metacaspases are not just biological oceanographers. Further physiological and biochemical-based observations, together with proteomics and mass spectrometry and future molecular study, eventually can help us develop a better understanding of these intriguing enzymes.